Discrete Local Volatility for Large Time Steps

(Extensive Version)

Hans Buehler, Evgeny Ryskin
QR Equities & Financing
JP Morgan Chase

Extensive Version 2.3, January 2015 - May 2016

Abstract

We construct a state-and-time discrete martingale which is calibrated *globally* to a set of given input option prices which may exhibit arbitrage.

We also provide an method to take small steps, fully consistent with the transition kernels of the large steps.

Its robustness vs. arbitrage violations in the input surface makes our approach particularly suited for computations in stressed scenarios. Indeed, our method of finding a *globally* closest arbitrage-free surface under constraints on implied and local volatility is useful in its own right.

While we do not aim at approximating a diffusion in our approach, our method may still be interpreted as a discrete version of Dupire's Local Volatility [Du96]. We will make this link explicit with the introduction of our "Backward Local Volatility".

This version of the paper is very extensive and provides much detail on how to construct our discrete martingale. A second, much more concise version is in preparation. The material discussed here was also presented at Global Derivatives 2016 [BG16] given

Contents

Version History

- V2.02: major rewrite from the original paper "Arbitrage-Free Fitting under bounds on Local and Implied Volatilities" which now also covers construction of transition probabilities.
- V2.03: added references to Derman-Kani [DK94] and fixed minor typos
- V2.04: rewrote section 4.3.3 and added a worked example for taking very large steps; fixed minor typos
- V2.05: minor updates
- V2.06: added examples of pricing Bermdan Digitals to illustrate model behaviour
- V2.07: fixed several typos and rewrote the introduction
- V2.08: reordered transition matrix discussion
- V2.09: fixed typos and added remarks 4.2 on page 27 and remark 4.3 on page 30. They simplify the representation of our transition matrices considerably (using directly densities and call prices, not Gamma or Theta),

but reduce its intuitive interpretation via local volatility. A link to the continuous case is also provided.

- V2.1: rewrote abstract and introduction, plus added a result on time interpolation
- V2.11: further clean up of notation; streamlined proofs of consistency for both explicit and implicit operators.
- V2.2: changed the title (again); reviewed the notion of transition probabilities (now called transition kernels) in view of our planned follow-up paper on stochastic volatility and jumps; added a comment on how to interpolate between arbitrage-free options in a way which maintains boundness of Backward Local Volatility (and also commented when a scheme for arbitrary intermediate strikes doesn't work)
- V2.21: We have fixed theorem 4.1 about the forward operator being the adjoint of the backward operator. We also addded with 3.1 an illustration of a case where Forward-Theta is positive, but the surface still exhibits arbitrage.
- V2.3: Following a discussion with Brian Huge we added multiple references to [AH10] which contains already many of the ideas presented here. We have also highlighted differences to their approach where applicable.
- V2.4: Amended small step decomposition.

1 Introduction

In this article, we present a method to calibrate globally a discrete time-and-space martingale to an observed or interpolated set of input option prices, which may or may not exhibit arbitrage.

Assume we are given a set of market observable option prices across maturities, including, possibly, some prices which are obtained by interpolation and extrapolation using an implied volatility fitting schema.

1. Find a *globally* closest model option price surface using linear programming for the input strikes and maturities.
2. Construct explicitly the transition kernels for a discrete martingale which reprices all our model option prices perfectly.

   No bootstrapping required.
3. Where needed, utilize our method of generating consistent small-step transition operators between the provided "large-step" maturities.

Accordingly, this article is split in two parts: in the first part, we cover the concept of absence of arbitrage over discrete strikes/maturities. The main contribution is an algorithm which allows finding globally an arbitrage-free surface

closest to an input surface. The L^1 version is an efficient linear program and can be used in the context of electronic market making or on-the-fly during risk and stress calculations. Its global nature means that it does not suffer from the limitations of common bootstrapping methods. This is an extension of our earlier work [Bu06] and is a useful contribution in its own right, in particular when pricing derivatives under Stress which might create artificial arbitrage in the stressed option surface.

The second part discusses how we can construct numerical pricing schemes which are fully consistent with our arbitrage-free surface, i.e. those which reprice our arbitrage-free call prices perfectly even when used with sparse grids and large time steps. We interpret our approach as a "sparse" version of Dupire's local volatility [Du96], which is also uniquely defined and which defines a discrete martingale process which "reprices" the arbitrage-free surface generated in the first step. To this end we are using implicit FD operators to construct transition matrices a'a Andreasen and Huge [AH10], and present a construction which works with any grid of strikes maturities. The ability to use an increasing range of strikes per maturity while keeping their number constant is particularly important as it allows an efficient use of time and space.

Moreover, in contrast to [AH10], we are not "bootstrapping" a diffusive local volatility by "recursively solving the forward system", since we already found a globally consistent surface in our first step. In fact, we do not at all look back to the diffusive case and remain in the discrete martingale setting.

Finally, we are also providing a means to take small steps between the reference maturities which are consistent with the respective calibrated transition kernels.

This paper is an extension of our earlier work "Expensive Martingales" [Bu06] where we presented a more convoluted form of the first step of finding a discrete arbitrage-free surface, and where the construction of transition kernels was not explicit, but was performed using linear programming under minimization of errors of pricing forward-started options.

1.1 Arbitrage-Free Surfaces

A common starting point for most valuation and risk management models in quantitative finance is the existence of a continuous set of option prices, which should be arbitrage-free in the sense that those prices do not exhibit any calendar- or butterfly-arbitrage plus some boundary conditions.

In practise, however, market prices are only observed at discrete strikes and maturities, and they are subject to bid/ask spreads, which means that any discrete set of "mid-prices" risks not leading to an arbitrage-free option surface. The market may also not be entirely consistent with our model assumptions, for example if we are trying to fit an equity derivative cash divided model to a market which exhibits only proportional dividends, c.f. [Bu10].

In order to obtain a continuous surface of option prices or, equivalently, implied volatilities, these "market prices" are then typically interpolated with

an "implied volatility model" which tends to be a heuristic interpolation and extrapolation scheme, for example a second-order log-moneyness interpolation or the SIV-inspired methodologies by Gatheral [Ga06]. It is one of the dark arts of practical finance to interpolate implied volatilities efficiently with a closed form scheme.

The optimal solution would be an implied volatility interpolation scheme which has easy-to-understand parameters, fits most real markets well, and does not require heavy numerical calibration. However, we are not aware of such a method. We therefore propose to first fit the observed market prices with an intuitive and fast, but possibly not arbitrage-free interpolation scheme, and to then take care of the arbitrage violations in a second step with a very efficient algorithm. The first part of this article presents such an algorithm:[1]

Given an input option price surface, we describe with result 3.1 a fast method of finding a global L^1-closest option price surface which is strictly arbitrage-free via linear programming.

This part of this note can be seen as a practical extension of our earlier work [Bu06]. We improve the clarity of the results somewhat, and remove the requirement in [Bu06] that the strikes at later maturities must contain those from earlier ones.

We also note that generating close arbitrage-free surfaces is a common task during stress and other risk calculations, and is a useful tool for electronic market making of European vanilla options.

1.2 Fully Consistent Pricing with Discrete Local Volatilities

For simple applications such as European option pricing or Vanilla option quoting systems, it is sufficient to have simply a surface of arbitrage-free option prices. However, for valuation and risk management of path-dependent products it is necessary to construct a martingale process which is "consistent" with the option surface in the sense that it reprices all vanilla option prices.

The classic approach is to use local volatility: given an arbitrage-free and sufficiently smooth surface of option prices $\mathbb{C}(t,k)$, Dupire's [Du96] famous local volatility is given as

$$\sigma_t^2(k) = 2\frac{\partial_t \mathbb{C}(t,k)}{k^2 \partial_{kk}^2 \mathbb{C}(t,k)} \ . \tag{1}$$

The solution to the SDE

$$\frac{dX_t}{X_t} = \sigma_t(X_t)\, dW_t$$

will then *fit* the input option market in the sense that $\mathbb{E}[(X_t - k)^+] = \mathbb{C}(t,k)$. This model can then be used in either induction (FD) or Monte Carlo (MC)

[1] Of course, it would be possible to fit a martingale model such as Heston [He93] or Bates [Ba96] against the market prices, in which case the resulting surface would be arbitrage-free by construction. However, in that case the parameters of the "interpolation" scheme become hard to understand, and therefore hard to trade.

methods to price those products which cannot be decomposed into European payoffs.

In practise, σ is computed by finely discretizing the strike/maturity space, and to then approximate (1) numerically. The main challenge is not just to avoid arbitrage in the option surface, but also to make sure that (1) does not explode or becomes imaginary; to this end, we present with result 3.2 a simple extension of our arbitrage-free fitting program to ensure that the discretized local volatility function remains bounded.

However, the overall continuous-time local volatility approach has a fundamental limitation: using the classic approximation of local volatility and subsequent application of MC and FD schemes does not yield a fully consistent pricing scheme: the discretization error between the theoretically perfect diffusion solution and the actual implementation gets worse with widening time and strike steps. That means that this approach cannot be used for large time steps (such as weeks) or sparse sets of strikes – in a perfect world, we wish to rather use FD and MC methods which are *fully consistent* with our calibrated surface in the sense that they yield exactly our calibrated option prices, regardless of the chosen strike/maturity grid.

We therefore present with result 4.1 an explicit constructive method of creating unique transition probabilities between arbitrage-free option prices by using an extended version of the implicit FD approach presented by Andreasen and Huge in [AH10], which can handle time-inhomogeneous, non-equidistant grids, and which does not need to "bootstrap" a solution by "recursively solve the forward system".

To this end, we will use a sufficiently defined discrete "Backward Local Volatility". This has the advantage that our method converges to the proper Dupire model as the strike/maturity grid increases in density, and therefore retains its intuitive features. In this sense, our Backward Local Volatility is the discrete version of Dupire's local volatility.

In its ambition for an explicit construction, our method is closely related to the construction of explicit trinomial or higher order trees in the spirit of Derman and Kani [DK94] The numerical complexity is that of computing the inverse of a tri-band matrix for every time step.

The model allows taking very large steps as is illustrated in a worked example in section 4.5. We will also show how to construct transition kernels for small steps, which are consistent with our large steps.

1.3 Main Contributions

1. **Arbitrage-Free Fitting with Bounds on Implied and Local Volatilities:** we present an efficient *global* arbitrage-free fitting scheme, which allows imposing bounds on both Dupire's "Forward" or our "Backward Local Volatility" – in other words, we do need to refer to bootstrapping our model iteratively forward. This makes this model particularly suited for calculations under Stress or other situations where arbitrage is likely to occur.

This is an efficient version of our earlier work [Bu06].

2. **Call-Price Preserving Interpolation of Densities:** we present an interpolation method for time-inhomogeneous grids which is a martingale transition matrix.

   This allows using an increasing strike grid while keeping the number of strikes constant across time without a decay in quality of fit – a major efficiency advantage over time-homogeneous grids.

   This is also of independent interest as a martingale implementation scheme for FD methods if the grid geometry changes over time.

3. **Discrete Local Volatility for Large Time Steps:** we show that using our "Backward Local Volatility" allows the efficient construction of transition matrices between maturities which are fully consistent, i.e. all option prices are recovered. This leads to fully consistent MC and FD schemes for pricing path-dependent payoffs.

   This is the same construction proposed in [AH10], but without the need for "recursively solving the forward system".

4. **Construction of Small Steps:** we present a simple method which allows the construction of transition operators for small time steps which are consistent with the large step operators.

1.4 Structure of the Approach

Let $\mathbb{C}_j^i$ be a set of market call prices for maturities $0 < t_1 < \cdots < t_m$ and strikes $0 \le k_j^{-1} < \cdots < 1 < \cdots < k_j^{n_j}$. We assume that the strikes at the boundary points are priced at intrinsic value, $C_j^{-1} = 1 - k_j^{-1}$ and $C_j^{n_{j-1}} = 0$.

Find the surface C closest to the input surface $\mathbb{C}$ which satisfies the following linear constraints:

1. $C_j^0 \ge 1 - k_j^0$,
2. $C_j^{n_j-1} \ge 0$,
3. $0 \le \Gamma_j^i$ defined as second order difference scheme for $i = 0, \ldots, n_j - 1$, and
4. Define $0 \le \not{b}\Theta_j^i := C_j^i - C_{j-1}(k_j^i)$ where $C_{j-1}(k_j^i)$ is defined as the linear interpolation of C_{j-1} at strike k_j^i.

   Then impose the linear constraint
   $\sigma_-^2 \ \frac{1}{2}\Gamma_j^i k_j^{i\,2} dt_j \le \not{b}\Theta_j^i \le \sigma_+^2 \ \frac{1}{2}\Gamma_j^i k_j^{i\,2} dt_j$ for $i = 0, \ldots, n_j - 1$,
   which also ensures that $\not{b}\Theta \ge 0$.

Then, "Backward Local Volatility"

$$\varsigma_j^i := \sqrt{2\frac{\not{b}\Theta_j^i}{\Gamma_j^i k_j^{i\,2} dt_j}}$$

is well-defined and bounded by σ_- and σ_+. The associated extended implicit FD operator with this Backward Local Volatility is a transition matrix consistent with the discrete marginal distribution implied by C, and can therefore be used for discrete Monte Carlo simulation or FD induction methods. Its transpose represents the implicit forward FD operator. We also discuss how to handle non-homogeneous grids.

The model is fully constructive in the sense that the most complex operation required is taking the inverse of a tri-band matrix when computing the implicit FD operator.

We also show in section 4.4 how to construct intermediate transition operators for small steps which integrate to the overall large step transition operators.

Thanks

We want to thank Nicolas Victoir for several good suggestions, in particular around the use of implicit operators for generating transition matrices.

2 Setup

We aim to model a martingale process X, e.g. the "pure" martingale of a stock price process[2] or any other tradable such as an FX rate. In particular, that means $1 = X_0 = \mathbb{E}[X_t]$ for all $t \geq 0$.

In the text below, we will use λ to refer to the Lebesgue-measure. We will also use the operator $x^+ := \max\{0, x\}$.

All vectors are assumed to be column vectors by default; we use a prime $'$ to denote the transpose. The elements of a matrix $M \in \mathbb{R}^{n,m}$ with m columns and n rows are indexed as usual by $M^{r,c}$ with row r and column c.

We make the following assumptions regarding the structure of our problem:

Maturities:
We assume we are given maturities $0 =: t_1 < \cdots < t_m < \infty$. We abbreviate $X_j := X_{t_j}$. The index letter j will be used throughout to refer to "time".

We also define $dt_j^+ := t_{j+1} - t_j$ and $dt_j^- := t_j - t_{j-1}$.

Strikes:
We refer to the n_j strikes of the jth maturity as $k_j = (k_j^{-1}, k_j^0, \ldots, k_j^{n_j})$ with $0 \leq k_j^{-1} < k_j^0 < k_j^{n_j}$; strikes are by construction relative to the martingale X of the

[2] In the case of equities, X can be defined as follows: assume $S = (S_t)_t$ is a stock prices model with deterministic forward $F = (F_t)_t$ and discount factors $\mathrm{DF} = (\mathrm{DF}_t)_t$. We assume that $X_t := S_t/F_t$ is a strictly positive martingale, which means that we effectively model dividends as proportional and consider credit risk as negligible; see [Bu10] on how to incorporate cash dividends or credit risk.

Given option prices on S, we can then extract "pure" option prices relative to X as follows: assume that $\mathcal{C}(T, K)$ is a call option on S with maturity T and strike K, then $\mathbb{C}(T, k) := \mathcal{C}(T, kF_T)/(\mathrm{DF}_T F_T)$ is a call on X with maturity T and relative strike k.

underlying asset, i.e. in practise defined in "forward space". We will use k_j to refer to the vector of all strikes at t_j.

Allowing arbitrary strikes per maturity means that common FD smoothing techniques such as placing grid points around discontinuities are well supported.

For numerical efficiency, we also require that

1. strikes span both sides of 1, i.e. $k_j^0 < 1$ and $1 < k_j^{n_j-1}$.[3]
2. the range of strikes widens, i.e.

$$k_j^{-1} \leq k_{j-1}^{-1} \quad \text{and} \quad k_j^{n_j} \geq k_{j-1}^{n_{j-1}} \tag{2}$$

   on downside and upside, respectively.[4]

For efficiency of exposure, we also define the "ghost" strikes

$$k_j^{-2} := k^{-1} - (k_j^0 - k_j^{-1}) \quad \text{and} \quad k_j^{n_j+1} := k^{n_j} + (k_j^{n_j} - k_j^{n_j-1}) \ .$$

Note that k_j^{-2} might be negative.

Options:
We denote by $\mathbb{C}_j^i := \mathbb{C}(t_j, k_j^i)$ for $j = 1, \ldots, m$ and $i = 0, \ldots, n_j - 1$ our input option prices. Note that we excluded the boundary strikes k_j^{-1} and $k_j^{n_j}$ which we will price at intrinsic value.

We aim to find a surface of call prices $C_j^i \equiv \mathbb{E}[(X_j - k_j^i)^+]$ for $j = 1, \ldots, m$ and $i = -1, \ldots, n_j$ which is closest to $\mathbb{C}$ but is arbitrage-free. Below we will impose a restriction that C_j^i is intrinsic for $i = -2, -1, n_j, n_j + 1$. This ensures that we can construct a discrete density which is consistent with the option prices, which has non-zero mass in the input strikes $k^{-1}, \ldots, k^{n_j}$.

Weights:
We are also given a set of positive weights $\omega = (\omega_j^i)_{(j,i)}$ for $j = 1, \ldots, m$ and $i = 0, \ldots, n_j - 1$ which are used to measure the penalty of not fitting an option price $\mathbb{C}_j^i$ with a fitted price C_j^i.

These weights define the L^1-weighted objective as

$$\Omega_1(C) := \sum_{j=1}^{m} \sum_{i=0}^{n_j-1} \omega_j^i |C_j^i - \mathbb{C}_j^i| \ . \tag{3}$$

Evidently, we may use any other L^p-metric to define optimality in (3), i.e.

$$\Omega_p(C) := \sqrt[p]{\sum_{j=1}^{m} \sum_{i=0}^{n_j-1} \omega_j^i |C_j^i - \mathbb{C}_j^i|^p} \ .$$

[3] If this condition does not hold, then the only arbitrage-free option prices for this maturity are those given by intrinsic call prices.

[4] If boundaries for a martingale are constant across time, then they become an absorbing state. In order to avoid this, we recommend a growing widths of the strike range. See also proposition 2.1 and the commentary afterwards for a motivation for (2).

Practically, we assume that market-observable options have much higher weights than those whose prices are generated by the implied volatility interpolation scheme described in the introduction.

A classic weighting scheme for the market-observable option prices is using the inverse of "Vega", in which case the penalty term per option in first order represents a mismatch in implied volatility. The author favours instead using a weighting inversely proportional to the bid/ask spread of the option price.

Volatility Bounds:
We are also given bounds on implied volatility $0 \leq \Sigma_- < \Sigma_+$ and local volatility $0 \leq \sigma_- < \sigma_+$ which we wish to impose.

In this context, we denote by $\mathrm{BS}_j^i(\Sigma)$ the Black-Scholes price of the call option with maturity t_j, strike k_j^i and volatility Σ. Naturally, we are more restrictive on implied than on local volatility, which i.e.

$$0 \leq \sigma_- \leq \Sigma_- < \Sigma_+ \leq \sigma_+ \ . \tag{4}$$

2.1 Absence of Arbitrage

Let us now introduce a few formal concepts to help with the discussion below. First of all, we will only search for optimal option prices C to match $\mathbb{C}$ within the boundary constraints for $\mathbb{C}$:

DEFINITION 2.1 *The set of* admissible *candidate price surfaces $C = (C_j^i)$, $j = 1, \ldots, m$ and $i = -1, \ldots, n_j$ is given by imposing intrinsic values at the strike boundaries:*

$$\mathcal{L}_* := \left\{ \ C \ : \ C_j^{-1} = 1 - k_j^{-1} \text{ and } C_j^{n_j} = 0 \text{ for } j = 1, \ldots, m \ \right\} \ . \tag{5}$$

We also set $C_0(k) := (1-k)^+$.

DEFINITION 2.2 (Absence of Arbitrage) *Let $C \in \mathcal{L}_*$.*

1. ***Maturity**: we call the strip C_j* arbitrage-free*, or the surface C* arbitrage-free at maturity t_j*, if there exists a non-negative random variable X_j with $\mathbb{E}[X_j] = 1$ such that*

$$C_j^i = \mathbb{E}[(X_j - k_j^i)^+] \quad \text{for all } i = -1, \ldots, n_j. \tag{6}$$

This is equivalent to the existence of a density p_j with $\int x p_j(x)\, dx = 1$ and $\int (x - k_j^i)^+ p_j(x)\, dx = C_j^i$.

2. ***Surface**: we call the surface C of call prices* arbitrage-free *if there exists a martingale $X = (X_j)_{j=0,1,\ldots,m}$ with $X_0 = 1$ such that*

$$C_j^i = \mathbb{E}[(X_j - k_j^i)^+] \quad \text{for all } j = 1, \ldots, m \text{ and } i = -1, \ldots, n_j. \tag{7}$$

We then say X fits *to C.*

From convexity it follows that

PROPOSITION 2.1 *Assume $C \in \mathcal{L}_*$ is arbitrage free at maturity t_j, i.e. (6) holds. Then, call prices on X_j outside its strike range have intrinsic value,*

$$C_j(k) := \mathbb{E}[(X_j - k)^+] = (1-k)^+ \text{ for } k \notin (k_j^{-1}, k_j^{n_j}) \ .$$

As a consequence, we may define consistently $C_j^{-2} := 1 - k_j^{-2}$ and $C_j^{n_j+1} := 0$.

REMARK 2.1 *This observation motivates (2): assume that (2) would not apply. Then, $\mathbb{P}[\ X_j \in [k_\ell^{-1}, k_\ell^{n_\ell}]\ \ell : \ell \geq j\ ]$, i.e. X_j is bounded by all future k_ℓ^{-1} and $k_\ell^{n_\ell}$, $\ell = j, \dots, m$. In other words, (2) simply ensures that all boundary points have a chance of being attainable. Removing (2) will not impede the theoretical conclusions presented below, but will diminish the numerical performance of our approach.*

Why not Time-Homogeneous Grids?

The above formalism around strikes and maturities is rather tedious, so one may well reasonably ask why we did not just focus on the case where strikes are the same per maturity, and maybe even equidistant.

The reason for that is that modelling martingales on a rectangular grid produces rather messy side effects. This is because for a martingale, a constant bound becomes an absorbing state. So let us say our strike range is fixed within $[k^{-1}, k^n]$. If the process ever hits k^{-1} or k^n, then it is stuck there - which in turn implies that the probability of reaching either point increases over time. This is self-evident noting that typically a classic diffusion model will grow of order $\sim e^{\sqrt{t}}$.

Practically, that means that when using rectangular grids, we have to use a wide range of strikes to avoid this effect creeping in.[5] For example, both [AH10] and [AH11] as presented share this drawback.

Hence, our requirement of increasing strikes (2).

An practical remedy is "Jordinson scaling",[6] i.e. to scale the process by its growth rate,or, equivalently, by providing a widening grid for the process

$$k_j^i = \exp\left\{\delta \frac{2(i+1) - (n+1)}{n+1} \Sigma\sqrt{t} - \frac{1}{2}\Sigma^2 t\right\} \tag{8}$$

where Σ denotes some implied volatility, and with a δ of around three, say. In that case, the boundary states keep increasing, thereby providing more room for the martingale to evolve. However, in order to use this one will need to define an interpolation scheme for the FD grid which is maintains the martingale property for the un-scaled process; standard spline methods, for example, will not suffice. We will present such a method in section 4.3.3.

[5] This is also why the boundary conditions for the density in forward PDE solvers are so complicated. Using Dirichlet leads to "loss of probability" while an absorbing boundary condition creates aforementioned accumulation effect.

[6] C.f. pages 59ff in our presentation [Bu11]

2.2 Linear Algebra for Options

The task at hand is to find a set of call prices $C \in \mathcal{L}_*$ which are minimal with respect to $\Omega(C)$, are arbitrage-free, and satisfy the provided bounds on implied and local volatility.

For our discussion, let us introduce a few intuitive linear operators on C. We fix j and define $dk_+^i := k_j^{i+1} - k_j^i$ and $dk_-^i := dk_+^{i-1} = k_j^i - k_j^{i-1}$.

Gamma – the second order approximation for the second derivative of C with respect to strike, *Gamma*, is on our non-equidistant grid given by

$$\Gamma_j^i := \gamma_j^{i-}\ C_j^{i-1} - 2\gamma_j^i\ C_j^i + \gamma_j^{i+}\ C_j^{i+1} \quad \text{for } i = -1, \dots, n_j. \tag{9}$$

with weights

$$\gamma_j^{i+} := \frac{2}{(dk_+^i + dk_-^i)dk_+^i}\ , \quad \gamma_j^i := \frac{1}{dk_+^i dk_-^i} \ \text{ and } \ \gamma_j^{i-} = \frac{2}{(dk_+^i + dk_-^i)dk_-^i} \tag{10}$$

(c.f. appendix A.1). *Note that Gamma is the second order derivative of the option price with respect to strike, not to spot.* Gamma is a linear function of C. Using our ghost strikes, Gamma is also defined for $i = -1$ and $i = n_j$.

Delta – we also define (upward) delta as

$$\Delta_j^i := \begin{cases} \frac{C_j^{i+1} - C_j^i}{dk_+^i} = \frac{C_j^{i+1} - C_j^i}{k_j^{i+1} - k_j^i} & : \ i = -1, \dots, n_j - 1\ , \\ 0 & : \ i = n_j\ . \end{cases} \tag{11}$$

Again, Delta is the first order derivative of the option price with respect to strike, not to spot. Note that

$$\Gamma_j^i = \frac{\Delta_j^i - \Delta_j^{i-1}}{\frac{1}{2}(dk_+^i + dk_-^i)} \tag{12}$$

is for $i = -1, \dots, n_j$.[7]

Linear Interpolation – for computing call prices for off-grid strikes, we will interpolate linearly. Outside our strike range, we impose extrapolate with intrinsic values:

$$C_j(k) := \begin{cases} \frac{k - k_j^{\ell-1}}{k_j^\ell - k_j^{\ell-1}} C_j^\ell + \frac{k_j^\ell - k}{k_j^\ell - k_j^{\ell-1}} C_j^{\ell-1} & k\ :\ k_j^{\ell-1} < k \le k_j^\ell\ , \\ 1 - k & k\ :\ k \le k^{-1}\ , \\ 0 & k\ :\ k \ge k^{n_j}\ . \end{cases} \tag{13}$$

[7] $\Delta_j^i - \Delta_j^{i-1} = \frac{dk_-^i (C_j^{i+1} - C_j^i) - dk_+^i (C_j^i - C_j^{i-1})}{dk_+^i dk_-^i} = \frac{1}{dk_+^i} C_j^{i+1} - \frac{dk_+^i + dk_-^i}{dk_+^i dk_-^i} C_j^i + \frac{1}{dk_-^i} C_j^{i-1}$

This is equivalent to assuming that the process X only takes values on the the strikes k_j with a density p_j, since then

$$\sum_{i:k_j^i>k} p_j^i(k_j^i - k) = C_j(k) \ .$$

Theta – for $j = 0, \ldots, m-1$ we define *Forward-Theta* as

$$f\Theta_j^i := C_{j+1}(k_j^i) - C_j^i$$

Backward-Theta is defined for $j = 1, \ldots, m$ equivalently as

$$b\Theta_j^i := C_j^i - C_{j-1}(k_j^i) \ ,$$

i.e. here we interpolate in t_{j-1}. Also recall that $C_0(k) = (1-k)^+$.

Both definitions of Theta are linear functions of C.

3 Arbitrage-Free Fitting with Bounds on Implied and Local Volatilities

We already made the following observation in [Bu06]:

THEOREM 3.1 (Absence of Arbitrage, one Maturity) *Let $C \in \mathcal{L}_*$. For a fixed maturity j assume that*

$$\Gamma_j^i \geq 0 \quad \textit{for } i = -1, \ldots, n_j. \tag{14}$$

Then C_j is arbitrage-free at maturity t_j.

The reverse is evidently also true, i.e. the existence of an X_j with (6) implies (14).

The above condition (14) is using the "ghost strikes" k_j^{-2} and $k_j^{n_j+1}$. If one wants to avoid using these, then the classic (equivalent) conditions of absence of arbitrage are

1. $C_j^0 \geq 1 - k_j^0$ (which is equivalent to $\Delta_j^{-1} \geq -1$),[8]
2. $C_j^{n_j-1} \geq 0$ (which is equivalent to $\Delta_j^{n_j-1} \leq 0$),[9] and
3. $\Gamma_j^i \geq 0$ for $i = 0, \ldots, n_j - 1$.

COROLLARY 3.1 *Define the density p_j for $j = 0, \ldots, m$ as*

$$p_j^i := \Delta_j^i - \Delta_j^{i-1} \equiv \frac{1}{2}(dk_+^i + dk_-^i)\Gamma_j^i \quad \textit{for } i = -1, \ldots, n_j. \tag{15}$$

Then, p_j fits C_j, i.e. satisfies (6).

We also note that $p_0(k) := 1_{k=0}$ is the density with unit mass in $k_0^0 = 1$.

[8] $\Delta_j^{-1} = (C_j^0 - C_j^{-1})/dk_+^{-1} = (C_j^0 - 1 + k_j^{-1})/dk_+^{-1} \geq (-dk_+^{-1})/dk_+^{-1} = -1$.

[9] $\Delta_j^{n_j-1} = (C_j^{n_j} - C^{n_j-1})/dk_+^{n_j-1} = -C^{n_j-1}/dk_+^{n_j-1} \leq 0$.

A related result is used in Derman/Kani [DK94] page 9ff. The proof for the above theorem and its corollary is provided in appendix A.2.

THEOREM 3.2 (Absence of Arbitrage, full Surface) *Assume that the assumptions of theorem 3.1 apply to all maturities $j = 1, \dots, m$. Assume in addition that*

$$b\Theta_j^i \geq 0 \quad \text{for } j = 2, \dots, m \text{ and } i = 0, \dots, n_j - 1. \tag{16}$$

(Note that by construction $b\Theta_1 \geq 0$ holds as well, and that $b\Theta_j^i = 0$ in all boundary strikes $i = -1, n_j$, too.)

Then, C is arbitrage-free*, and there exists a discrete martingale X with marginal distributions $p = (p_j)_j$ as defined in corollary 3.1.*

Again, the reverse is also true, i.e. any martingale with a marginal distribution p which satisfies (7) will satisfy conditions (14) and (16), too.

This was proven in [Bu06]. The existence of a martingale is equivalent to the existence of a martingale kernel, in the sense defined in the following section.

3.1 Transition Operators

DEFINITION 3.1 *We call a matrix M a* probability matrix *if its columns are probability densities, i.e. $1'M = 1'$ and $M \geq 0$.*

We say it has the martingale property *over two vectors of strikes k_1 and k_2 if*

$$k_2'M = k_1' \ .$$

In this case, we refer to M as a martingale kernel *(over k_1 and k_2).*

A particular useful fact to this end is the following observation which was made in [AH11]:

THEOREM 3.3 (Construction of Transition Matrices) *Assume that M is a square matrix with columns [rows] add up to 1, and all whose off-diagonal elements are non-positive.*

Then, its inverse exists, is non-negative, and its columns [rows] add up to 1; in other words M^{-1} is a probability matrix.

Moreover, if M has the martingale property with respect to k_2 and k_1, then M^{-1} has the martingale property with respect to k_1 and k_2.

Given the central role this theorem plays we sketch its proof: a matrix M with the above properties is evidently column-dominant (i.e. $M^{i,i} > \sum_{i \neq \ell} |M^{\ell,i}|$) and a Z-matrix (i.e. $M^{i,i} > 0$ and $M^{i,\ell} \leq 0$ for $i \neq \ell$). This means it is a non-singular M-matrix ([BR94], chapter 6: equivalent classification I_{29} of non-singular M-Matrices) and as such its inverse exists and is non-negative ([BR94], chapter 6: equivalent classification N_{38} of non-singular M-Matrices).

Finally, $1'M = 1'$ implies $1' = 1'M^{-1}$, i.e. the rows of M^{-1} add up to 1, too. Similarly, if $k_2'M = k_1'$, then $k_2' = k_1'M^{-1}$. □

DEFINITION 3.2 *Let $C \in \mathcal{L}_*$ be arbitrage-free and denote by $p = (p_j)_j$ the associated marginal densities.*

We call $\Pi_j \in \mathbb{R}^{n_j+2, n_{j-1}+2}$ a (consistent) transition matrix *from p_{j-1} to p_j if it is a probability matrix, and if*

$$p_j = \Pi_j p_{j-1}$$

holds.

We also call Π_j a (consistent) transition kernel *if it has additionally the martingale property over k_{j-1} and k_j.*

We call a sequence of matrices $\Pi = (\Pi_j)_{j=1,\dots,m}$ with $\Pi_j \in \mathbb{R}^{n_j+2,\, n_{j-1}+2}$ a martingale representation *(of C) if each Π_j is a transition kernel from p_{j-1} to p_j.*

In our discussion we may drop the word "consistent" if this requirement is obvious from the context.

THEOREM 3.4 *The existence of a martingale representation for C kernel is (tautologically) equivalent to the existence of a discrete martingale X which fits C, and which only takes values on our strike/maturity grid.*

A transition kernel Π_j is a matrix which has to satisfy the linear conditions listed in definition 3.2: positivity, probability, martingale-property and consistency with p. Hence, in order to find a suitable Π_j, we have to solve a linear program. However, since the solution space is very large,[10] this approach is not satisfactorily for a general purpose fast pricing scheme.[11] We would much rather have a direct method to construct uniquely defined transition kernels which also provides some intuitive interpretation. We will present such a method based on FD operators in section 4: we will show that implicit or explicit FD operators of forward-PDEs are actually consistent transition kernels.

Residual Results

PROPOSITION 3.1 *If C is arbitrage-free, then Forward-Theta is also non-negative.*

Note that the reverse relationship does not hold: imposing $f\Theta^i_j \geq 0$ instead of *4.* is not sufficient for showing absence of arbitrage on a non-homogeneous grid. Figure 3.1 shows an example where Forward-Theta is positive for all 3M strikes, while the surface is visibly not arbitrage-free. Backward-Theta at 4M is negative, accordingly.

[10] Any candidate matrix has $\sim n^2$ elements, but is subject to only $\sim 3n$ constraints. In [Bu06] we therefore propose defining an optimal choice among all possible matrices by minimizing the pricing error of exotic options, for example forward-started vanillas.

[11] In [Bu06] we have used linear programming to find transition kernels which closest reprice forward started options. However, that method is not very fast.

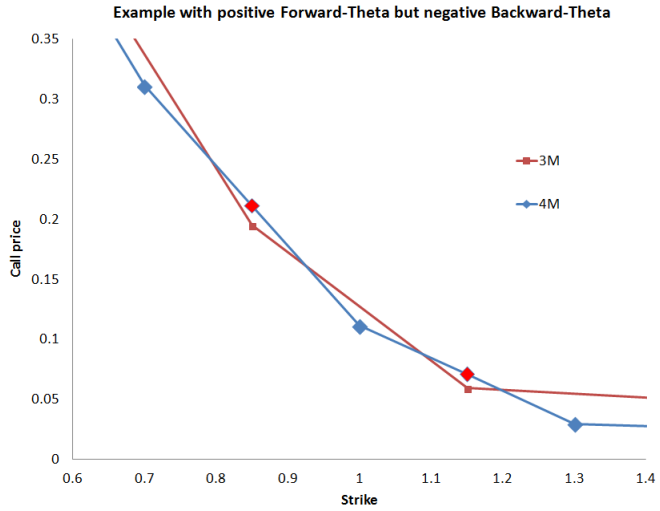

The following was proven before in [Bu06]:

THEOREM 3.5 (Expensive Martingales) *The discrete martingale X above is a "most expensive" martingale which fits C in the sense that if Z is another martingale which fits C, then $\mathbb{E}[f(X_j)] \geq \mathbb{E}[f(Z_j)]$ for all convex functions f and all t_j.*

This also means that $b\Theta_j^i = 0$ on the boundary points $i = -1, n_j$.

It is trivial to show that for any X which fits C, for all strikes on the grid,

- $f\Theta$ is an upper bound for analytic Forward-Theta,
- $b\Theta$ is a lower bound for analytic Backward-Theta,[12] and
- Γ_j^i is an upper bound for analytic Gamma.

The next paragraphs will discuss practical means to construct arbitrage-free option price surfaces. The construction of a martingale representation for C is then presented in section 4 on page 22.

3.2 Bounds on Implied Volatility

Recall that $\mathrm{BS}_j^i(\Sigma)$ denotes the Black-Scholes price of a call option with maturity t_j, strike k_j^i and volatility Σ.

DEFINITION 3.3 *We denote by $\mathcal{L}_0$ the set of admissible call prices $C \in \mathcal{L}_*$ which satisfy 1.-4. above, and which are bounded by $\mathrm{BS}_j^i(\Sigma_-) \leq C_j^i \leq \mathrm{BS}_j^i(\Sigma_+)$.*

[12] Note that if *4.* holds, then Backward-Theta is positive for all strikes, not just those in k_j: Linear interpolation of C_j over k_j dominates all other convex functions f with $f(k_j^i) \leq C_j^i$. For strikes outside $[k_j^{-1}, k_j^{n_j}]$, our requirement of an increasing domain and that we extrapolate with intrinsic values ensures a non-negative Backward-Theta.

Since we can always chose $C_j^i = \mathrm{BS}_j^i(\Sigma_-)$ it follows trivially that:

PROPOSITION 3.2 *The affine set $\mathcal{L}_0$ is non-empty.*

RESULT 3.1 *A solution to*

$$\mathrm{argmin}_{C\in\mathcal{L}_0}\Omega(C)$$

is an Ω-optimal fit to $\mathbb{C}$ under implied volatility constraints.

This program therefore implements finding an arbitrage-free set of option prices with simple linear programming.

3.3 Bounds on Forward Local Volatility

We now aim to impose a restriction on (classic) local volatility. If the time step $dt_j^+ = t_{j+1} - t_j$ is sufficiently small, and the strikes are close to each other, then we may approximate Dupire's local volatility function (1) by discritization as

$$\sigma_j^{i\,2} := 2\frac{f\Theta_j^i}{k_j^{i\,2} dt_j^+ \ \Gamma_j^i} \quad \text{if } \Gamma_j^i > 0, \text{ or 0 otherwise} \tag{17}$$

for $j = 0, \ldots, m-1$ and $i = 0, \ldots, n_j - 1$. We call this definition of local volatility *Forward Local Volatility* since we are using Forward-Theta for the time decay component.

We may now restrict our solution space to those call prices which admit a bounded local volatility – the following is the first main result of this article:

RESULT 3.2 (Fitting under Local and Implied Volatility Bounds) *Let*

$$\mathcal{L}_f := \left\{ C \in \mathcal{L}_0 : \ \sigma_-^2 \ \frac{1}{2} k_j^{i\,2} dt_j^+ \ \Gamma_j^i \le f\Theta_j^i \le \sigma_+^2 \ \frac{1}{2} k_j^{i\,2} dt_j^+ \ \Gamma_j^i \,; \ \begin{matrix} j = 0, \ldots, m-1; \\ i = -1, \ldots, n_j \end{matrix} \right\}. \tag{18}$$

A solution to the program

$$\mathrm{argmin}_{C\in\mathcal{L}_f}\Omega(C) \tag{19}$$

is an Ω-optimal arbitrage-free fit to $\mathbb{C}$ under both local and implied volatility constraints for Forward Local Volatility.

The program (19) therefore implements finding an arbitrage-free set of option prices with bounds on local and implied volatility to a set of observable and interpolated option prices using linear programming.

It should be noted that as it stands, there is no guarantee that $\mathcal{L}_f$ is non-empty for all choices of implied and local volatility bounds, even if (4) is true. This is because the local volatility formula (17) is just an approximation: assume, for example, that $\sigma_- = \Sigma_- = \Sigma_+ = \sigma_+ =: \Sigma$, meaning the only possible solution at an infinitesimal grid for (19) is the option price surface generated by Black&Scholes at an implied volatility of Σ. However, by increasing the time step of the discretization (17) we can make Forward-Theta arbitrarily large,

hence its upper bound in (18) will be violated. On the other hand, by increasing the distance between the strikes we can increase Gamma, which in turn will lead to a violation of the lower bound on Theta.

The authors would welcome results on when $\mathcal{L}_f$ is non-empty for given implied and local volatility bounds.

Backward

Equation (17) uses Forward-Theta to approximate our local volatility. That is the classic approach derived from the explicit formulation of the forward-PDE for the call prices. However, as we saw above, it is positivity of Backward-Theta which determines absence of arbitrage. We therefore may define (discrete) *Backward Local Volatility* as

$$\varsigma_j^{i\,2} := 2\frac{b\Theta_j^i}{\Gamma_j^i k_j^{i\,2} dt_j^-} \quad \text{if } \Gamma_j^i > 0, \text{ or 0 otherwise,} \tag{20}$$

for $j = 1, \ldots, m$ and $i = -1, \ldots, n_j$ with $dt_j^- = t_j - t_{j-1}$.[13] Note that Backward-Theta and therefore our Backward Local Volatility is by construction zero in the boundary points k_j^{-1} and $k_j^{n_j}$, because call prices there are intrinsic in both t_j and t_{j-1}.

Boundness of Backward Local Volatility is imposed within the affine set

$$\mathcal{L}_b := \left\{ C \in \mathcal{L}_0 : \ \sigma_-^2 \ \frac{1}{2} k_j^{i\,2} dt_j^- \ \Gamma_j^i \le b\Theta_j^i \le \sigma_+^2 \ \frac{1}{2} k_j^{i\,2} dt_j^- \ \Gamma_j^i ; \quad \begin{matrix} j = 1, \ldots, m; \\ i = 0, \ldots, n_j - 1 \end{matrix} \right\} . \tag{21}$$

RESULT 3.3 *A solution to*

$$\text{argmin}_{C \in \mathcal{L}_b} \Omega(C) \ . \tag{22}$$

is an Ω-optimal arbitrage-free fit to $\mathbb{C}$ under implied and local volatility constraints for use of Backward Local Volatility.

We want to stress that (22) represents a globally optimal fit to the input surface, in contrast to iterative methods which use forward FD's; c.f. our own work [Bu11] and the references therein, or Andreasen and Huge [AH10], [AH11].

Note that of the two constraints on Backward Local Volatility the upper bound is most critical. It basically ensures that whenever Backward Theta is non-zero, that Gamma is non-zero, too, such that (20) is well-defined.

We will also see in the next section that ensuring boundness of Backward Local Volatility is a more natural choice than using Forward Local Volatility, since the former ensures that the implicit forward-FD operator is a consistent transition kernel for C.

[13] Recall that $C_0(k) := (1-k)^+$.

3.4 Examples

We illustrate the algorithm with a few examples.

First graph shows the algorithm applied to a surface with intentional random error terms:

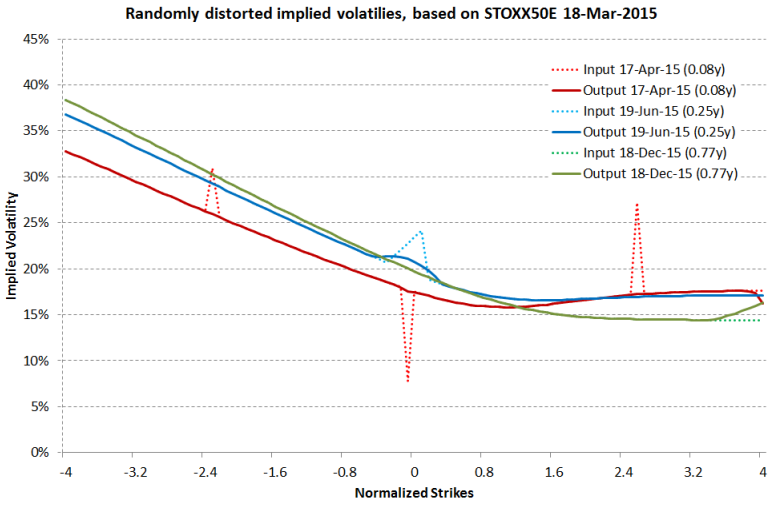

2

The next example shows how the algorithm fixes real arbitrage violations. The graph shows a few selected maturities of a fit to an mismarked surface.

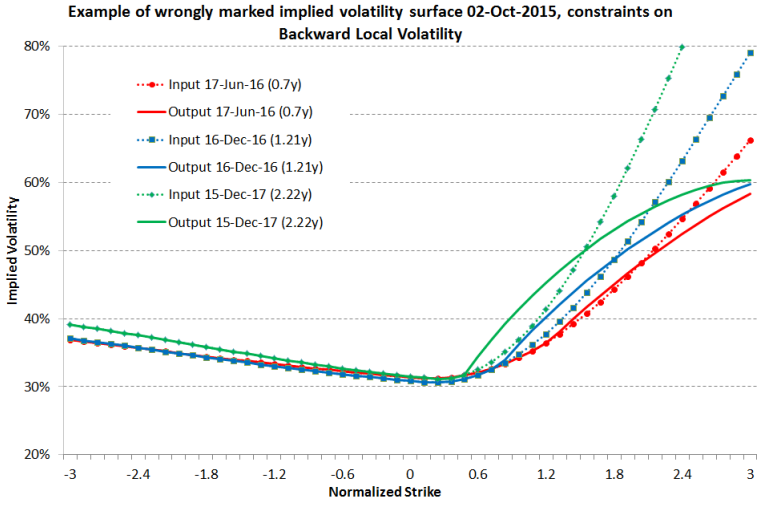

An Extreme Example

We now illustrate the algorithm on an extreme example. The input implied volatility and local volatility surfaces are given as follows:

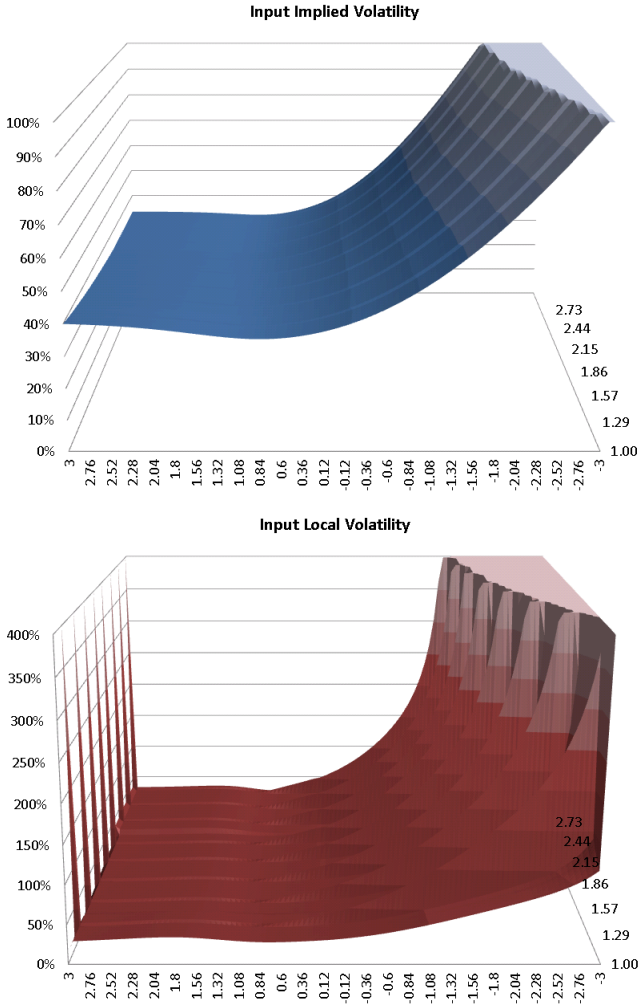

local volatility does not exist on the right hand side extreme strikes (which is mapped to +1000).

We now our apply Backward Local Volatility calibration with a lower bound of 5% and an upper bound of 300%. The result is:

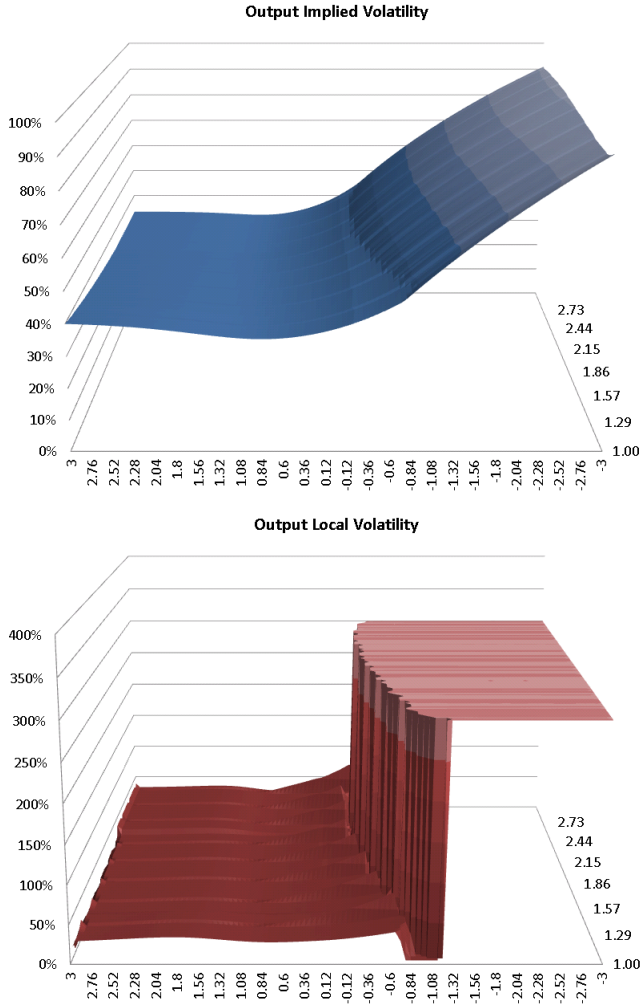

We see that even with an extreme local volatility of 300% we can not fit the input implied volatility.

Numerical Effects

It is notable that an upper bound on local volatility, in particular Forward Local Volatility easily becomes binding. The follwing graph shows one maturity of an arbitrage-free fit, as a function of Forward local volatility upper bound.

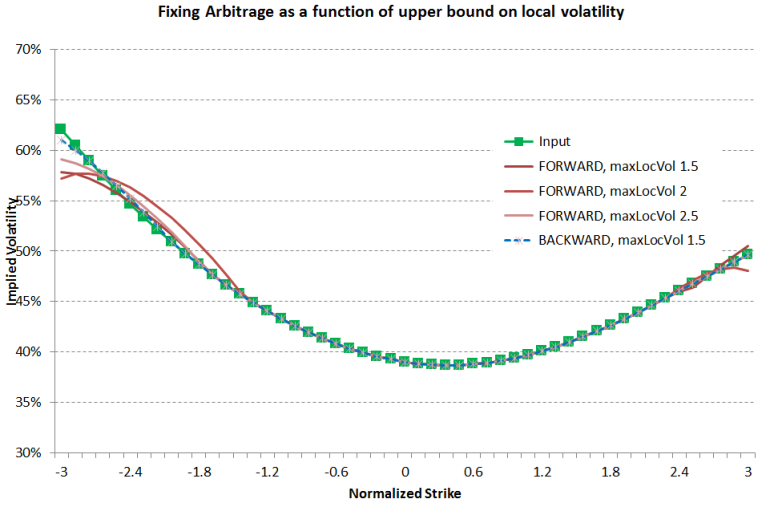

The fit on the left hand side does not match the input surface for $\sigma_+ = 150\%$, but it does when this limit is raised to 300%. The Backward Local Volatility program fits even with 150%.

4 Fully Consistent Pricing with Discrete Local Volatilities

In the previous section we have shown how to find an Ω-closest option surface to the input surface $\mathbb{C}$ with bounds on implied volatility and, mechanically, on local volatility when the latter is computed off our strike grid.

However, what is not clear is that even with such a bounded local volatility, an FD or MC scheme using it actually produces our call price values C. The issue is that definitions (17) and (20), respectively, are discrete approximations of a continuous problem. In particular if we have a sparse grid (for example with time-steps several weeks wide), the corresponding Monte-Carlo or FD methods will not recover our European option prices C due to discretization errors – even if local volatility is bounded. In fact, this will certainly not be the case if we naively sample normal variables dW to drive the associated SDE $dX_t = X_t \sigma_t(X_t)\, dW_t$ over wide time steps. A discussion on discretization errors for diffusions can be found in Kloeden/Platen [KP11].

DEFINITION 4.1 *We call a numerical scheme* $\tilde{E} : f \mapsto \tilde{E}[f(X)]$ fully consistent *with* C *if*

$$\tilde{E}[(X_j - k_j^i)^+] = C_j^i \quad \textit{for all } j = 0, \dots, m \textit{ and } i = -1, \dots, n_j$$

analytically (ie, barring implementation issues such as rounding errors).

In fact, this problem is closely related with the production of martingale representation for C in the sense of definition 2.2. Assume that $\Pi = (\Pi_j)_j$ is such a representation. In that case, dynamic programming for a terminal payoff F can be implemented fully consistently with C as the program

$$\left\{ \begin{array}{lcll} f_m & := & F(k_m) & j \ : \ j = m \\ f_j & := & f'_{j+1}\,\Pi_{j+1} & j \ : \ j = 0, \ldots, m-1 \ , \end{array} \right.$$

where each vector f_j has values $f_j^i = \mathbb{E}[F(X_T)|X_j = k_j^i]$ with in particular $f_0 = \mathbb{E}[F(X_T)]$.

Similarly, a Monte-Carlo forward method can be implemented easily by sampling from the transition kernels: let F_j be the conditional distribution probability matrix with $F_j^{(\ell|i)} := \mathbb{E}[X_j \leq k_j^\ell | X_{j-1} = k_{j-1}^i]$, and denote by $F_j^{-1}(\cdot|k_j^i)$ its left-inverse. Assume that $u = (u_j)_{j=1,\ldots,m}$ is an iid series of uniform variables; then,

$$\left\{ \begin{array}{lcll} X_0 & := & 1 & \\ X_j & := & F_j^{-1}(u_j|X_{j-1}) & j \ : \ j = 1, \ldots, m \end{array} \right.$$

implements a fully consistent Monte-Carlo simulation scheme.

It should be noted that if we have access to the explicit transition operators, then the model lends itself to Likelihood Ratio greek calculations. Assume, for example, that $\Pi^* = (\Pi_j^*)_j$ is the martingale representation for our model under a perturbation of one of the market inputs. To compute the "perturbed" price of a payoff H, we may simply evaluate under the same above scheme the new payoff

$$H^*(x_1, \ldots, x_m) := H(x_1, \ldots, x_m) \prod_{j=1}^{m} \frac{\Pi_j^*(x_j|x_{j-1})}{\Pi_j(x_j|x_{j-1})} \ .$$

Figure 4 illustrates the power of this method.

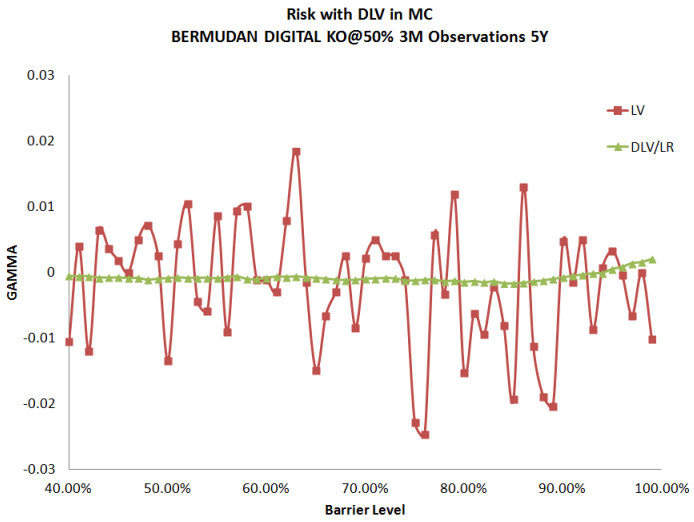

4.1 Transition Kernels and FD schemes

In order to generate consistent transition kernels, we will establish linear conditions on our problem such that not only local volatility exists but also that the respective FD operators yield directly unique transition kernels. The resulting program therefore finds a Ω-optimal fit under the condition that our FD operators generate a consistent transition kernel. Our approach is an extension of Andreasen and Huge's implicit FD method [AH10] to arbitrary grids.

To motivate our approach, recall the forward PDE for a density of a local volatility martingale,

$$\partial_t p_t(k) = \frac{1}{2}\partial^2_{kk}\left\{\sigma_t^2(k)k^2\, p_t(k)\right\} \ . \tag{23}$$

In order to solve such a problem, we discretize the operator such that

$$p_{t+dt} = p_t + L^i_t p_{t+dt} + L^e_t p_t$$

(note that p_{t+dt} is the unknown). In other words

$$p_{t+dt} = U_t p_t \ , \quad U_t := (1 - L^i_t)^{-1}(1 + L^e_t) \ .$$

Hence, we want to understand when U_t is actually a transition kernel.

Backward and Forward

Instead of working directly with (23), we want to make use of the duality between forward and backward PDEs. To this end, assume that the density of our process X vanishes outside a compact set, for example our strike range.

Assume that $f_t(x) := \mathbb{E}[f(X_T)|X_t = x]$ for a convex function f with compact support. Then, it solves the backward PDE

$$-\partial_t f_t(x) = \frac{1}{2}\sigma_t^2(x)x^2\ \partial^2_{xx} f_t(x) \tag{24}$$

We discretize the backward operator as

$$f_t = W_t f_{t+dt} \ , \quad W_t := (1 - H^i_t)^{-1}(1 + H^e_t) \tag{25}$$

(here, f_t is the unknown). We observe that for any convex f with compact support, in operator notation,

$$f'_{t+dt}p_{t+dt} = \mathbb{E}[f(X_T)] = f'_t p_t = (f_{t+dt}W_t)'p_t = f'_{t+dt}(W'_t p_t) \ .$$

Since f was arbitrary, this means that

$$p_{t+dt} = W'_t p_t \quad \lambda\text{-a.s.} \tag{26}$$

As is proven in appendix A.2, more generally we have:

THEOREM 4.1 *The backward operator of a diffusion with unattainable boundaries (i.e. a diffusion whose forward PDE for its density does has Neumann boundaries) is the adjoint (i.e. transpose) of its forward operator.*

See also the comments around equations (20) and (20) in [AH11].

Since W_j is the backward FD operator, we usually know by construction that its rows add up to one ($1 = W_t 1$) and that it has the martingale property ($k_j = W_t k_{j+1}$). Hence, as long as we can show that W_j is non-negative, we can generate transition kernels for p as transposes of operators for backward PDE's.

In Andreasen and Huge's article [AH11] these properties are used in a two-factor stochastic volatility setting.

REMARK 4.1 (Andreasen-Huge [AH11]) *We want to make a few comments towards Andreasen and Huge's work [AH11]. There, it was stated that*

1. *On Backward and Forward FD approximations:*
   "The approximations are not mutually consistent. Specifically, direct application of the same type of finite difference scheme to (2) and (3) would not lead to the same results." *[below equation (7)]*

   This is just an effect of expanding analytically the derivative term in (24) into first and second derivatives on σ and p. As formulated in (24), discrete forward and backward FD schemes are the exact transpose of each other. This was used in [Bu11].

2. *On boundary conditions for the backward scheme:*
   "there is no need to take special care of the boundary conditions at the edges because these are implicitly defined by the backward scheme." *[below equation (17)]*

   The "implicitly" defined boundary conditions for the scheme proposed in [AH11] on a time-homogeneous grid are the same as the ones used here – which means that for a constant grid, the boundaries become absorbing and "pile up" probabilities.

4.2 Explicit Transition Kernels

To gain some intuition, we start with the simple case of a fixed set of equidistant strikes, used homogeneously across time, and an explicit FD scheme. This section is for illustration only and the keen reader may proceed directly with section 4.3 on page 27.

In this section, we assume $C \in \mathcal{L}_f$.

The classic explicit backward FD scheme for a function f which vanishes outside our strike range $k^{-1}, \dots, k^n$ is given as

$$f^i_{j-1} = f^i_j + w^i_j \left(f^{i+1}_j - 2 f^i_j + f^{i-1}_j \right) \tag{27}$$

with

$$w^i_j := \frac{1}{2} {\sigma^i_j}^2 {k^i}^2 \frac{dt_+}{dk^2} \ , \quad i = -1, \dots, n$$

where σ is our Forward Local Volatility. On our time-homogeneous grid, Forward Local Volatility is zero at the boundary points.

Most notably, $w_j^i \geq 0$. We have

$$w_j^i = \frac{f\Theta_j^i}{\Gamma_j^i}\frac{1}{dk^2} = \frac{C_{j+1}^i - C_j^i}{C_j^{i-1} - 2C_j^i + C_j^{i+1}} \ , \quad i = -1, \ldots, n \ .$$

Recall from corollary 3.1 that $p_j^i = \frac{1}{dk}\left(C_j^{i-1} - 2C_j^i + C_j^{i+1}\right)$ which gives

$$w_j^i = \frac{1}{dk}\frac{C_{j+1}^i - C_j^i}{p_j^i} \ , \quad i = -1, \ldots, n \ . \tag{28}$$

Since $C \in \mathcal{L}_f$, this is well-defined with the convention $0/0 = 0$. The associated explicit backward operator is given by the triangular matrix

$$\begin{pmatrix} 1 & 0 & & & \\ w_j^0 & 1-2w_j^0 & w_j^0 & & \\ & \ddots & \ddots & \ddots & \\ & & w_j^{n-1} & 1-2w_j^{n-1} & w_j^{n-1} \\ & & & 0 & 1 \end{pmatrix} \ .$$

The adjoint forward FD is

$$p_{j+1}^i = p_j^i + \left(w_j^{i+1}p_j^{i+1} - 2w_j^i p_j^i + w_j^{i-1}p_j^{i-1}\right) \ . \tag{29}$$

which is represented by the transpose of the above matrix as

$$E_{j+1} := \begin{pmatrix} 1 & w_j^0 & & & \\ 0 & 1-2w_j^0 & & & \\ & w_j^0 & \ddots & w_j^{n-1} & \\ & & & 1-2w_j^{n-1} & 0 \\ & & & w_j^{n-1} & 1 \end{pmatrix} \ .$$

It is straight forward to see that this is a martingale kernel if and only if $1-2w_j^i \geq 0$, i.e. $w_j^i \leq \frac{1}{2}$.

It remains to show that E_{j+1} is also consistent. Assume that we have solved the forward FD (29) for p until t_j. We want to show that

$$p_{j+1} = E_{j+1}p_j \ .$$

The forward FD gives us for $i = 0, \ldots, n$

$$\begin{aligned} (E_{j+1}p_j)^i &= p_j^i + \left\{w_j^{i+1}p_j^{i+1} - 2w_j^i p_j^i + w_j^{i-1}p_j^{i-1}\right\} \\ &\overset{(28)}{=} p_j^i + \frac{1}{dk}\left\{C_{j+1}^{i+1} - 2C_{j+1}^i + C_{j+1}^{i-1}\right\} - \frac{1}{dk}\left\{C_j^{i+1} - 2C_j^i + C_j^{i-1}\right\} \\ &= p_j^i + (p_{j+1}^i - p_j^i) \ = \ p_{j+1}^i \ , \end{aligned}$$

hence E_{j+1} is indeed a consistent transition kernel.

PROPOSITION 4.1 *Assume that $C \in \mathcal{L}_f$ and in addition that*

$$C_{j+1}^i - C_j^i \leq \frac{1}{2}\left(C_j^{i-1} - 2C_j^i + C_j^{i+1}\right) \ . \tag{30}$$

Then, the explicit operator E_{j+1} over a homogeneous equidistant grid is a transition kernel for C, i.e.

$$p_j = E_j p_{j-1} \ .$$

When seen over the grid of a trinomial tree, this gives us a necessary and sufficient condition for the feasibility of using the tree with the standard explicit pricing scheme. Derman/Kani [DK94] try to alleviate this restriction by allowing the nodes of the tree to move, which provides more freedom to fit the input option price surface.

REMARK 4.2 *Note that we have shown above that the ith column of the explicit forward operator can simply be written as*

$$\left(\cdots\ 0\ ,\ \frac{1}{dk}\frac{C_{j+1}^{i-1} - C_j^{i-1}}{p_j^{i-1}}\ ,\ 1 - \frac{2}{dk}\frac{C_{j+1}^i - C_j^i}{p_j^i}\ ,\ \frac{1}{dk}\frac{C_{j+1}^{i+1} - C_j^{i+1}}{p_j^{i+1}}\ ,\ 0\ ,\cdots \right)' . \tag{31}$$

In fact, this result can also be derived Dupire-like way for diffusions:

Let $dX_t = X_t \sigma_t(X_t)\, dW_t$. As usual,

$$\partial_t C_t(x) = \frac{1}{2}\sigma_t^2(x)x^2\partial_{xx}^2 C_t(x) = \frac{1}{2}\sigma_t^2(x)x^2 p_t(x) \ . \tag{32}$$

Differentiation yields the forward PDE for the density,

$$\partial_t p_t(x) = \frac{1}{2}\partial_{xx}^2\Big\{\sigma_t^2(x)x^2 p_t(x)\Big\}$$

Using (32) to replace the volatility term gives

$$dp_t(x) = \partial_{xx}^2 \frac{dC_t(x)}{p_t(x)}\, p_t(x) \ ,$$

i.e. the continuous version of (31).

4.3 Implicit Transition Kernels

We have seen that explicit FD operators can provide consistent transition kernels, but also that in order to do so, we have to impose an additional linear constraint (30) on our linear program (19).

We will now show that this is not the case for implicit FD operators. As an illustration, we first discuss the equidistant case since it is easier to follow, and then expand to the general case for arbitrary grids.

In this section, we assume that $C \in \mathcal{L}_b$.

4.3.1 Time-Homogeneous Equidistant Grid

We assume again that we use equidistant strikes, used homogeneously across maturities. The classic implicit backward FD scheme for a function f which vanishes outside our strike range is given as

$$f_j^i - w_j^i(f_j^{i+1} - 2f_j^i + f_j^{i-1}) = f_{j+1}^i$$

with weights defined as

$$w_j^i := \frac{1}{2}\varsigma_j^{i2}k^{i2}\frac{dt_-}{dk^2} \ .$$

Here, we used Backward Local Volatility ς as defined in (20). This gives

$$w_j^i = \frac{b\Theta_j^i}{\Gamma_j^i}\frac{1}{dk^2} = \frac{1}{dk}\frac{C_j^i - C_{j-1}^i}{p_j^i}$$

for $i = -1, \ldots, n$, which is well-defined for $C \in \mathcal{L}_b$. Since C is at intrinsic value in the boundary strikes, we have again $w_j^i = 0$ for $i = -1, n-1$. The implicit forward FD operator is given by the inverse of the triangular matrix

$$I_j^{-1} = \begin{pmatrix} 1 & -w_j^0 & & & \\ 0 & 1+2w_j^0 & -w_j^1 & & \\ 0 & -w_j^0 & \ddots & -w_j^{n-1} & \\ & & & 1+2w_j^{n-1} & 0 \\ & & & -w_j^{n-1} & 1 \end{pmatrix} \ .$$

This is the same operator as the transpose of A defined in (10) in [AH10]. Note that here we have systematically motivated the choice of the absorbing boundary conditions by enforcing that the call prices there are priced at intrinsic.

The conditions of theorem 3.3 apply, hence *without further conditions*, I_j exists and is a transition kernel.

It remains to show that it is also consistent, i.e. $p_j = I_j p_{j-1}$. Since I_j^{-1} is invertible, it is sufficient to show that $I_j^{-1}p_j = p_{j-1}$. We define for notational convenience $w_j^{-2} = w_j^{n+1} := 0$ such that we can write for $i = -1, \ldots, n$:

$$\begin{aligned} (I_j^{-1}p_j)^i &= p_j^i - \frac{1}{dk}p_j^{i-1}w_j^{i-1} + \frac{2}{dk}p_j^i w_j^i - \frac{1}{dk}p_j^{i+1}w_j^{i+1} \\ &= p_j^i - \frac{1}{dk}\left\{C_j^{i+1} - 2C_j^i + C_j^{i-1}\right\} + \frac{1}{dk}\left\{C_{j-1}^{i+1} - 2C_{j-1}^i + C_{j-1}^{i-1}\right\} \\ &= p_{j-1}^i \ . \end{aligned}$$

This shows indeed that I_j is consistent.[14]

[14] Without using our ghost strikes, we can show directly that we have the following at the lower boundary: $p_{j-1}^{-1} = q_j^{-1} - \frac{1}{dk}b\Theta_j^{i+1}\frac{q_j^{i+1}}{p_j^{i+1}} \overset{(*)}{=} \ldots = q_j^{-1} - \left\{(\Delta_j^{-1}+1) - (\Delta_{j-1}^{-1}+1)\right\} = p_{j-1}^{-1}$. The upper boundary can be shown in a similar way.

PROPOSITION 4.2 *Assume that $C \in \mathcal{L}_b$.*
Then, then the implicit operator I_j over a homogeneous equidistant grid is (unconditionally) a transition kernel for C.

4.3.2 Time-Homogeneous Non-Equidistant Grids

We now relax the assumption on strikes being equidistant, but still assume that our strikes $k = (k^i)_i$, $0 \leq k^{-1} < \cdots < 1 < \cdots k^n$ are used homogeneously across maturities. The main result of this section is simply to show that proposition 4.2 also holds for non-equidistant strikes. Readers who agree with this right away may proceed directly to section 4.3.3 on page 30 where discuss general non-homogeneous grids.

Backward Local Volatility over a non-equidistant grid is given by

$$\varsigma_j^{i\,2} := \frac{b\Theta_j^i}{\frac{1}{2}k^{i2}dt_j^-\ \Gamma_j^i}\ .$$

For $C \in \mathcal{L}_b$ the above is well-defined with $0/0 := 0$.

The implicit backward FD scheme on k for a function which f vanishes outside that strike range is given by

$$f_j^i - \left(w_j^{i+} f_j^{i+1} - 2w_j^i f_j^i + w_j^{i-} f_j^{i-1}\right) = f_{j+1}^i \tag{33}$$

with non-negative weights

$$w_j^{i\cdot} := \frac{1}{2}\varsigma_j^{i\,2} k_j^{i\,2}\ dt_j^- \gamma_j^{i\cdot} = \frac{b\Theta_j^i}{\Gamma_j^i}\gamma_j^{i\cdot} \overset{(15)}{=} \frac{C_j^i - C_{j-1}^i}{p_j^i}\bar{\gamma}_j^{i\cdot}\ , \tag{34}$$

where we define

$$\bar{\gamma}_j^{i\cdot} := \frac{1}{2}(dk_+^i + dk_-^i)\gamma_j^{i\cdot} \tag{35}$$

using the γ weights defined in (10) as

$$\gamma_j^{i+} := \frac{2}{(dk_+^i + dk_-^i)dk_+^i}\ ,\quad \gamma_j^i := \frac{1}{dk_+^i dk_-^i}\ \text{ and }\ \gamma_j^{i-} = \frac{2}{(dk_+^i + dk_-^i)dk_-^i}\ .$$

As before, we note that at the boundary points $i = -1, n$ we have $b\Theta_j^i = 0$ and therefore $w_j^i = 0$. Let I_j again be the inverse of the implicit forward operator, i.e.

$$I_j^{-1} = \begin{pmatrix} 1 & -w_j^{0-} & & & \\ 0 & 1 + 2w_j^0 & & & \\ & -w_j^{0+} & \ddots & -w_j^{(n-1)-} & \\ & & & 1 + 2w_j^{(n-1)} & \\ & & & -w_j^{(n-1)+} & 1 \end{pmatrix}\ . \tag{36}$$

Since $w_j^{i-} - 2w_j^i + w_j^{i+} = 0$, theorem 3.3 applies, hence the inverse if I_j^{-1} exists and is a martingale kernel.

It remains to show consistency with C. As before, invertibility of I_j means that we only have to show that $p_j I_j^{-1} = p_{j-1}$ holds. We obtain

$$\begin{aligned}(p_j I_j^{-1})^i &= p_j^i - \bar{\gamma}_j^{(i+1)-}\left(C_j^{i+1} - C_{j-1}^{i+1}\right) + 2\bar{\gamma}_j^i\left(C_j^i - C_{j-1}^i\right) - \gamma_j^{(i-1)+}\left(C_j^{i-1} - C_{j-1}^{i-1}\right) \\ &= p_{j-1}^i \ ,\end{aligned}$$

which shows consistency.

PROPOSITION 4.3 *Assume that $C \in \mathcal{L}_b$.*
Then, the implicit operator I over a time-homogeneous grid is (unconditionally) a transition probability for C.

REMARK 4.3 *Similar to the expression (31) for the explicit case we have just shown that the ith column inverse of the implicit forward operator can simply be written as*

$$\left(\cdots\ 0\ ,\ -\bar{\gamma}_j^{(i-1)+}\frac{C_j^{i-1} - C_{j-1}^{i-1}}{p_j^{i-1}}\ ,\ 1 + 2\bar{\gamma}_j^i\frac{C_j^i - C_{j-1}^i}{p_j^i}\ ,\ -\bar{\gamma}_j^{(i+1)-}\frac{C_j^{i+1} - C_{j-1}^{i+1}}{p_j^{i+1}}\ ,\ 0\ ,\cdots \right)' .$$

Writing this again in diffusion terms, we obtain the following implicit PDE for the density p of a local volatility diffusion

$$\begin{aligned}p_{t-dt}(x) &= \left\{1 - \partial_{xx}^2\left(\tfrac{1}{2}\varsigma_t(x)^2 x^2\right)\right\} p_t(x) \\ &= p_t(x) - \partial_{xx}^2\frac{C_t(x) - C_{t-dt}(x)}{p_t(x)}\, p_t(x)\end{aligned}$$

(here, p_t is the unknown).

4.3.3 Implicit Transition Kernels on General Grids

We now discuss the case of time-inhomogeneous grids. The main idea we propose is that in order to move forward a density p from time t_{j-1} defined on k_{j-1} to t_j over k_j, we first use p_{j-1} to obtain interpolated call prices $\tilde{C}_{j-1}$ at strikes k_j plus two additional ghost strikes. We then re-define a density $\tilde{p}_{j-1}$ using our standard probability formula (15) over k_j. The joint operation

$$\Xi_j \ : \ \tilde{p}_{j-1} = \Xi_j p_{j-1}.$$

is linear, but generally not invertible. This interpolation scheme maintains the martingale property between different strike grids k_{j-1} and k_j and ensures that the density after interpolation still adds up to one. This scheme is a contribution in itself.

The resulting $\tilde{p}_{j-1}$ is a density over k_j, hence moving to p_j has become a time-homogeneous problem which we can solve using the results of the previous section 4.3.2. Using the respective implicit FD operator I_j we obtain

$$p_j = \Pi_j p_{j-1}\ , \quad \Pi_j := I_j \Xi_j\ ,$$

i.e. Π_j is a consistent transition kernel.

Following the program we just laid out, assume that we have solved our density forward to t_{j-1}, with p_{j-1} defined on k_{j-1}. Using (13) we define intermediate call prices $\tilde{C}_{j-1}$ on $k^{-2}, k^{-1}, \dots, k^{n_j}, k^{n_j+1}$ as

$$\tilde{C}^i_{j-1} := \sum_{\ell=-1}^{n_{j-2}} p^\ell_{j-1} \omega^{i,\ell}_j \ , \quad \omega^{i,\ell}_j := \left(k^\ell_{j-1} - k^i_j\right)^+ \ , \tag{37}$$

where $\Omega_j = (\omega^{i,\ell}_j)$ for $i = -2, \dots, n_j + 2$ and $\ell = -1, \dots, n_{j-1}$ is a semi-upper triangular $\mathbb{R}^{n_j+4,\, n_j+2}$-matrix such that

$$\tilde{C}_{j-1} = \Omega_j p_{j-1} \ .$$

Schematically it has the form

$$\Omega_j \approx \begin{pmatrix} (k^{-1}_{j-1} - k^{-2}_j)^+ & (k^0_{j-1} - k^{-2}_j)^+ & \cdots & (k^{n_{j-1}}_{j-1} - k^{-2}_j)^+ \\ (k^{-1}_{j-1} - k^{-1}_j)^+ & (k^0_{j-1} - k^{-1}_j)^+ & \cdots & (k^{n_{j-1}}_{j-1} - k^{-1}_j)^+ \\ \vdots & & \ddots & \vdots \\ 0 & \cdots & \cdots & (k^{n_{j-1}}_{j-1} - k^{n_j}_j)^+ \\ 0 & 0 & \cdots & (k^{n_{j-1}}_{j-1} - k^{n_j+1}_j)^+ \end{pmatrix} \ .$$

The next step is to derive the intermediate density $\tilde{p}_{j-1}$ over k_j from $\tilde{C}_{j-1}$. Using (15) we find

$$\tilde{p}^i = \frac{dk^{i-1}_+ \tilde{C}^{i+1} - (dk^i_+ + dk^{i-1}_+)\tilde{C}^i + dk^i_+ \tilde{C}^{i-1}}{dk^i_+ dk^{i-1}_+} \quad i = -1, \dots, n_j \ ,$$

which is well-defined because of our use of the strikes k^{-2} and k^{n_j+1}. This yields in matrix notation

$$\tilde{p}_{j-1} = \Psi_j \tilde{C}_{j-1}$$

with

$$\Psi_j := \begin{pmatrix} \frac{1}{dk^{-2}} & -\frac{dk^{-1}+dk^{-2}}{dk^{-1}dk^{-2}} & \frac{1}{dk^{-1}} & & & & \\ & \frac{1}{dk^{-1}} & -\frac{dk^0+dk^{-1}}{dk^0 dk^{-1}} & \frac{1}{dk^0} & & & \\ & & \ddots & \ddots & \ddots & & \\ & & & \frac{1}{dk^{n-2}} & -\frac{dk^{n-1}+dk^{n-2}}{dk^{n-1}dk^{n-2}} & \frac{1}{dk^{n-1}} & \\ & & & & \frac{1}{dk^{n-1}} & -\frac{dk^n+dk^{n-1}}{dk^{n-1}dk^n} & \frac{1}{dk^n} \end{pmatrix} \ .$$

We define the joint operator as

$$\Xi_j := \Psi_j \Omega_j \ .$$

The map $\Xi_j : p_{j-1} \mapsto \tilde{p}_{j-1}$ is non-negative by construction: any positive p_{j-1} will yield a convex $\tilde{C}_{j-1}$, which is intrinsic at the boundary and ghost strikes.

This in turn yields a non-negative $\tilde{p}_{j-1}$. We also note that $k'_j \Xi_j = k'_{j-1}$ and that $1'\Xi_j = 1'$.[15]

The map Ξ is therefore a transition kernel. Hence, we obtain the second main result of this article:

RESULT 4.1 (Discrete Local Volatility) *Let C^* be a solution to*

$$C^* = \operatorname{argmin}_{C \in \mathcal{L}_b} \Omega(C) \ . \tag{38}$$

Then $(\Pi_j)_j$ with $\Pi_j := I_j \Xi_j$ is a consistent martingale kernel for C.

This result achieves the second stated objective of this article, i.e. to provide an efficient arbitrage-free fitting scheme, (38), whose solution C^* exhibits a consistent martingale kernel which can be constructed with basic algebra.

4.4 Small Steps

Let us assume that our model has been calibrated to options $C \in \mathcal{L}_b$ defined at observable market expiry dates $0 = t_0 < t_1 < \cdots < t_m$. This allows pricing path-dependent products whose payoffs depend on the values of the underlying equity at those expiries. However, this leaves open how we might price options which depend on intermediary time steps. Obviously, we may simply calibrate our model to finer time-steps, but in this case the "finer" model will have different transition probabilities between t_{j-1} and t_j than our original model – and it will be much slower to calibrate. Using always the "finer" model perturbs the idea of (fast) "large step" calibration filled with small steps. This deficiency is also shared with the proposed interpolation scheme in [AH10], equation (6).

We therefore present a numerically less costly approach which "fills" the overall transition operator with small operators, consistently with big step operator.

Let us first have a closer look at the tridiagonal matrix I_j^{-1}:

$$I_j^{-1} = \begin{pmatrix} 1 & -w_j^{0-} & & & \\ 0 & 1 + 2w_j^0 & & & \\ & -w_j^{0+} & \ddots & -w_j^{(n-1)-} & \\ & & & 1 + 2w_j^{(n-1)} & \\ & & & -w_j^{(n-1)+} & 1 \end{pmatrix} . \tag{39}$$

Denote the submatrix of I_j^{-1} formed by removing the first and the last rows and columns by $inner(I_j^{-1})$. Let us assume that off-diagonal elements of I_j^{-1} are non-zero. Indeed if any off diagonal element, say $w_j^{(m)+}$, is zero then so is

[15] $k'_j \Psi_j = \left(k^{-1} \frac{1}{dk^{-2}},\ -k^{-1}(\frac{1}{dk^{-2}} + \frac{1}{dk^{-1}}) + k^0 \frac{1}{dk^{-1}},\ 0, \ldots, 0,\ k^{n_j} \frac{1}{dk^{n_j - 1}} - k^{n_j - 1}(\frac{1}{dk^{n_j - 1}} + \frac{1}{dk^{n_j - 2}}),\ k^{n_j} \frac{1}{dk^{n_j}} \right)$.
$(k'_j \Psi_j \Omega_j)^\ell = (k^\ell_{j-1} - k_j^{-2}) k^{-1} \frac{1}{dk^{-2}} + (k^\ell_{j-1} - k_j^{-1}) \left\{ -k^{-1}(\frac{1}{dk^{-2}} + \frac{1}{dk^{-1}}) + k^0 \frac{1}{dk^{-1}} \right\} =$
$k^\ell_{j-1} \left(k^{-1} \frac{1}{dk^{-2}} - k^{-1} \frac{1}{dk^{-2}} - k^{-1} \frac{1}{dk^{-1}} + k^0 \frac{1}{dk^{-1}} \right) + k^{-1} \frac{k^{-1} - k_j^{-2}}{dk^{-2}} - k_j^{-1} \frac{k^0 - k^{-1}}{dk^{-1}} = k^\ell_{j-1}$

$w_j^{(m)-}$, in this case we shall remove the corresponding row-column from I_j^{-1} when forming the submatrix. Notice now that matrix $inner(I_j^{-1})$ is a real tridiagonal matrix with $a_{i,i+1}a_{i+1,i} = w_j^{(i)+}w_j^{(i+1)-} > 0$ for all i, therefore this matrix is similar to a Hermitian matrix i.e.

$$inner(I_j^{-1}) = P^{-1}HP$$

where H is a Hermitian matrix. Indeed, let P be a diagonal matrix with diagonal elements δ_i given by

$$\delta_0 = 1, \delta_i^2 = \frac{w_j^{0+}w_j^{1+}\dots w_j^{(i-1)+}}{w_j^{1-}w_j^{2-}\dots w_j^{i-}}, i = 1, \dots, n-1$$

H is then given by

$$H = \begin{pmatrix} 1+2w_j^0 & -\sqrt{w_j^{1-}w_j^{0+}} & & & \\ -\sqrt{w_j^{1-}w_j^{0+}} & 1+2w_j^1 & & & \\ & & \ddots & & \\ & & & 1+2w_j^{(n-2)} & -\sqrt{w_j^{(n-1)-}w_j^{(n-2)+}} \\ & & & -\sqrt{w_j^{(n-1)-}w_j^{(n-2)+}} & 1+2w_j^{(n-1)} \end{pmatrix}. \tag{40}$$

Since $inner(I_j^{-1})$ is similar to a real Hermitian matrix its eigenvalues are real. As shown in the proof of theorem 3.3 $inner(I_j^{-1})$ is also a non-singular M-matrix therefore its eigenvalues are actually positive. Let us denote n positive eigenvalues of $inner(I_j^{-1})$ as follows

$$\lambda_1, ..., \lambda_n$$

and n corresponding eigenvectors

$$v_1^{(inner)}, \dots, v_n^{(inner)}$$

The characteristic polinomial $P_{I_j^{-1}}(\lambda)$ of the original matrix I_j^{-1} can be decomposed into

$$P_{I_j^{-1}}(\lambda) = (1-\lambda)^2 P_{inner(I_j^{-1})}(\lambda)$$

therefore I_j^{-1} has two additional eigenvalues

$$\lambda_0 = \lambda_{n+1} = 1$$

with two additional eigenvectors

$$v_0 = (1, 0, \dots, 0)', \ v_{n+1} = (0, \dots, 0, 1)'$$

The eigenvalues of $inner(I_j^{-1})$ generate n eigenvectors for I_j^{-1} in the form

$$v_i = (0, (v_i^{(inner)})', 0)',\ i = 1, \ldots, n$$

Notice that $(v_i | i = 0, \ldots, n+1)$ are linearly independent and thus form a basis of the linear space with dimention $n+2$. This proves that I_j^{-1} (and its inverse I_j) has eigendecomposition with positive eigenvalues.

To this end, we may decompose I_j into

$$I_j = U_j D_j U_j^{-1}$$

where U_j is a matrix formed from eigenvectors I_j and D_j is a diagonal matrix whose elements are the eigenvalues of I_j. In our case this decomposition is particularly straight forward as I_j^{-1} is tridiagonal.

We may now define the transition operator for the step from $\tau_{\ell-1}$ to τ_ℓ as

$$\hat{I}_\ell := U_j D_j^{\frac{\tau_\ell - \tau_{\ell-1}}{t_j - t_{j-1}}} U_j^{-1}\ . \tag{41}$$

I_j is a transition kernel over strikes k_j which means that

$$1' I_j = 1',\ k_j' I_j = k_j$$

i.e. 1 and k_j are eigenvectors of I_j with unit eigenvalues therefore we have

$$1' \hat{I}_\ell = 1',\ k_j' \hat{I}_\ell = k_j'$$

which proves $\hat{I}_\ell$ is also a transition kernel over the same strikes k_j.

Evidently,

$$I_j = \prod_{\ell=1}^{L} \hat{I}_\ell\ . \tag{42}$$

Figure 4.4 illustrates how the grid geometry for our model. Basically, after each reference maturity (in black), the grid is extended to the strikes of the next maturity.

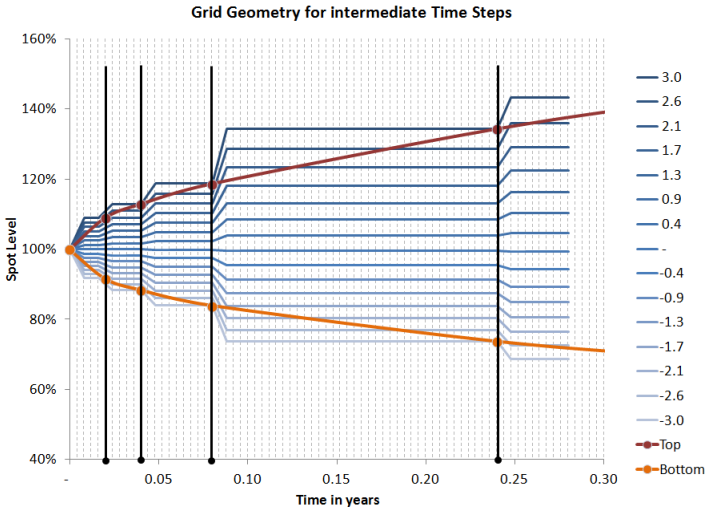

4.5 Worked Example: Calibration

To illustrate our algorithm to generate transition kernels, we use $n = 20$ and assume that our option prices for $t_1 = 3M = 0.25$ and $t_2 = 6M = 0.5$ are given by a Black&Scholes model with volatility $\Sigma = 20\%$. Define the 22 strikes by (8) with $\delta = 3$. We then compute European option prices using Black&Scholes' formula for all inner strikes, and set the boundary values to intrinsic. We obtain

the strikes

$$k_{3M} = \begin{pmatrix} 0.74 \\ 0.76 \\ 0.78 \\ 0.80 \\ 0.83 \\ 0.85 \\ 0.87 \\ 0.90 \\ 0.93 \\ 0.95 \\ 0.98 \\ 1.01 \\ 1.04 \\ 1.07 \\ 1.10 \\ 1.13 \\ 1.16 \\ 1.20 \\ 1.23 \\ 1.27 \\ 1.31 \\ 1.34 \end{pmatrix}, \; C_{3M} = \begin{pmatrix} 0.26 \\ 0.24 \\ 0.22 \\ 0.20 \\ 0.17 \\ 0.15 \\ 0.13 \\ 0.11 \\ 0.09 \\ 0.07 \\ 0.05 \\ 0.04 \\ 0.02 \\ 0.02 \\ 0.01 \\ 0.01 \\ 0.00 \\ 0.00 \\ 0.00 \\ 0.00 \\ 0.00 \\ 0.00 \end{pmatrix} \text{ and } \; k_{6M} = \begin{pmatrix} 0.65 \\ 0.67 \\ 0.70 \\ 0.73 \\ 0.76 \\ 0.79 \\ 0.83 \\ 0.86 \\ 0.89 \\ 0.93 \\ 0.97 \\ 1.01 \\ 1.05 \\ 1.10 \\ 1.14 \\ 1.19 \\ 1.24 \\ 1.29 \\ 1.34 \\ 1.40 \\ 1.45 \\ 1.51 \end{pmatrix}, \; C_{6M} = \begin{pmatrix} 0.35 \\ 0.33 \\ 0.30 \\ 0.27 \\ 0.24 \\ 0.21 \\ 0.18 \\ 0.15 \\ 0.12 \\ 0.10 \\ 0.07 \\ 0.05 \\ 0.04 \\ 0.02 \\ 0.01 \\ 0.01 \\ 0.00 \\ 0.00 \\ 0.00 \\ 0.00 \\ 0.00 \\ 0.00 \end{pmatrix}$$

The resulting densities for $3M$ and $6M$ are very similar, given that we scaled the grid with the native Black&Scholes kernel. We also provide the intermediate

density $\tilde{p}_{3M}$, defined on k_{6M}.

$$p_{3M} = \begin{pmatrix} 0.003 \\ 0.002 \\ 0.006 \\ 0.012 \\ 0.021 \\ 0.034 \\ 0.050 \\ 0.069 \\ 0.088 \\ 0.103 \\ 0.112 \\ 0.112 \\ 0.103 \\ 0.088 \\ 0.069 \\ 0.050 \\ 0.033 \\ 0.021 \\ 0.012 \\ 0.006 \\ 0.002 \\ 0.004 \end{pmatrix}, \quad \tilde{p}_{3M} = \begin{pmatrix} 0.000 \\ 0.000 \\ 0.000 \\ 0.003 \\ 0.005 \\ 0.012 \\ 0.033 \\ 0.053 \\ 0.094 \\ 0.131 \\ 0.143 \\ 0.172 \\ 0.124 \\ 0.106 \\ 0.063 \\ 0.034 \\ 0.018 \\ 0.005 \\ 0.004 \\ 0.000 \\ 0.000 \\ 0.000 \end{pmatrix} \quad \text{and} \quad p_{6M} = \begin{pmatrix} 0.003 \\ 0.002 \\ 0.006 \\ 0.012 \\ 0.021 \\ 0.034 \\ 0.050 \\ 0.069 \\ 0.088 \\ 0.103 \\ 0.112 \\ 0.112 \\ 0.103 \\ 0.088 \\ 0.069 \\ 0.050 \\ 0.033 \\ 0.021 \\ 0.012 \\ 0.006 \\ 0.002 \\ 0.004 \end{pmatrix}.$$

The three densities are shown in the following graph, where we also see the effect of the extrapolation from p_{3M} to $\tilde{p}_{3M}$:

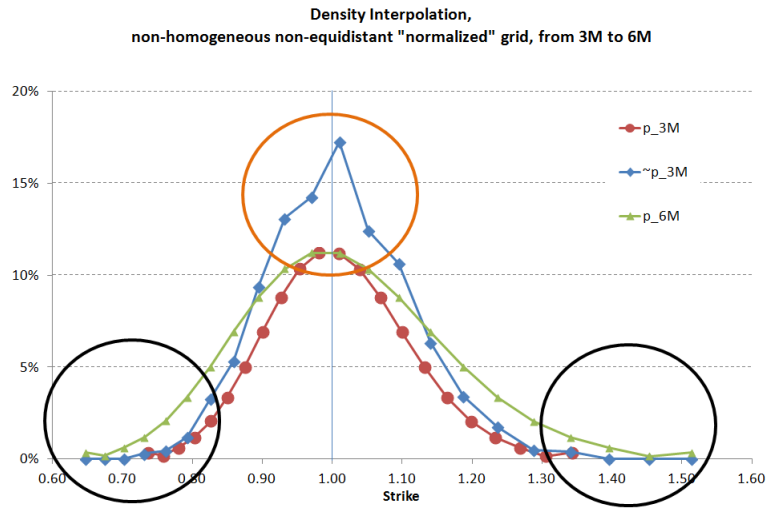

The black circles mark the strikes of k_j which are outside k_{j-1} and which therefore are assigned zero probability in $\tilde{p}_{j-1}$. The brown circle, on the other hand,

shows the residual interpolation arising from Ξ_j due to the lower density of strikes in k_j than k_{j-1} around ATM. All densities add up to one.

The next graph shows the call prices with respect to these probabilities. It illustrates well the concept of linear interpolation in call prices:

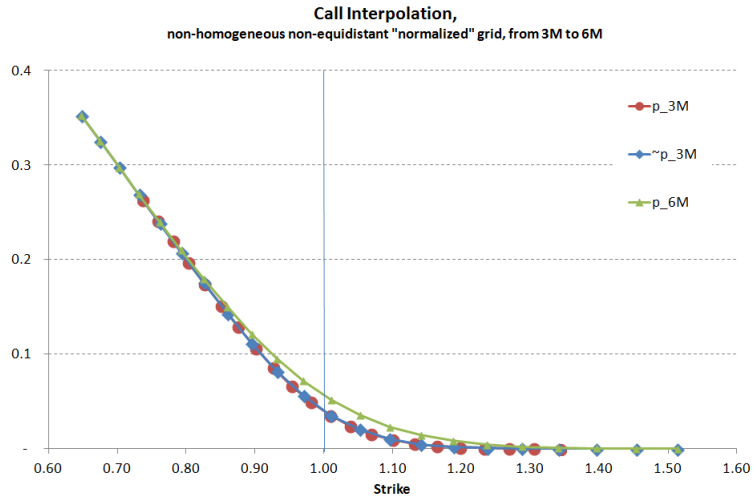

Finally, we show the joint transition kernel Π_{6M} from p_{3M} to p_{6M}.

	0.74	0.76	0.78	0.80	0.83	0.85	0.87	0.90	0.93	0.95	0.98	1.01	1.04	1.07	1.10	1.13	1.16	1.20	1.23	1.27	1.31	1.34
0.65	10%	6%	4%	2%	2%	1%	1%	1%	0%	0%	0%	0%	0%	0%	0%	0%	0%	0%	0%	0%	0%	0%
0.67	5%	3%	2%	1%	1%	1%	0%	0%	0%	0%	0%	0%	0%	0%	0%	0%	0%	0%	0%	0%	0%	0%
0.70	17%	11%	7%	4%	3%	2%	1%	1%	1%	0%	0%	0%	0%	0%	0%	0%	0%	0%	0%	0%	0%	0%
0.73	33%	20%	13%	8%	5%	4%	3%	2%	1%	1%	1%	0%	0%	0%	0%	0%	0%	0%	0%	0%	0%	0%
0.76	19%	33%	25%	16%	10%	7%	5%	3%	2%	2%	1%	1%	1%	0%	0%	0%	0%	0%	0%	0%	0%	0%
0.79	8%	14%	26%	28%	18%	12%	8%	6%	4%	3%	2%	1%	1%	1%	0%	0%	0%	0%	0%	0%	0%	0%
0.83	4%	7%	12%	20%	30%	21%	14%	9%	7%	5%	3%	2%	2%	1%	1%	0%	0%	0%	0%	0%	0%	0%
0.86	2%	3%	6%	10%	15%	25%	23%	16%	11%	8%	5%	4%	3%	2%	1%	1%	1%	0%	0%	0%	0%	0%
0.89	1%	2%	3%	5%	8%	13%	20%	25%	18%	12%	9%	6%	4%	3%	2%	1%	1%	1%	0%	0%	0%	0%
0.93	1%	1%	2%	3%	4%	7%	11%	16%	24%	20%	14%	10%	7%	5%	3%	2%	1%	1%	1%	0%	0%	0%
0.97	0%	0%	1%	1%	2%	4%	6%	9%	13%	21%	23%	16%	11%	8%	5%	3%	2%	1%	1%	1%	0%	0%
1.01	0%	0%	0%	1%	1%	2%	3%	5%	8%	12%	17%	25%	18%	12%	8%	6%	4%	2%	2%	1%	1%	0%
1.05	0%	0%	0%	0%	1%	1%	2%	3%	5%	7%	10%	15%	22%	22%	14%	10%	7%	4%	3%	2%	1%	1%
1.10	0%	0%	0%	0%	0%	1%	1%	2%	3%	4%	6%	9%	13%	19%	25%	17%	11%	7%	5%	3%	2%	1%
1.14	0%	0%	0%	0%	0%	0%	1%	1%	2%	2%	4%	5%	8%	12%	17%	25%	21%	14%	8%	5%	3%	2%
1.19	0%	0%	0%	0%	0%	0%	0%	1%	1%	1%	2%	3%	5%	7%	10%	15%	23%	26%	16%	11%	6%	4%
1.24	0%	0%	0%	0%	0%	0%	0%	0%	1%	1%	1%	2%	3%	4%	6%	9%	13%	20%	30%	21%	13%	7%
1.29	0%	0%	0%	0%	0%	0%	0%	0%	0%	0%	1%	1%	2%	2%	3%	5%	7%	11%	17%	28%	28%	16%
1.34	0%	0%	0%	0%	0%	0%	0%	0%	0%	0%	0%	1%	1%	1%	2%	3%	4%	6%	9%	14%	23%	34%
1.40	0%	0%	0%	0%	0%	0%	0%	0%	0%	0%	0%	0%	0%	1%	1%	1%	2%	3%	5%	7%	12%	19%
1.45	0%	0%	0%	0%	0%	0%	0%	0%	0%	0%	0%	0%	0%	0%	0%	0%	1%	1%	1%	2%	3%	5%
1.51	0%	0%	0%	0%	0%	0%	0%	0%	0%	0%	0%	0%	0%	0%	1%	1%	1%	2%	3%	4%	7%	11%

4.5.1 Large Steps

Let us also illustrate how the algorithm deals with large steps, where most of the strikes of t_j are outside the range of k_{j-1}. As an example we use exponentially-scaled strikes again defined by (8), but this time for $t_{j-1} = 3M$ and $t_j = 20Y$. Predictably, most of the density p_{3M} is mapped to a very simplified $\tilde{p}_{3M}$:

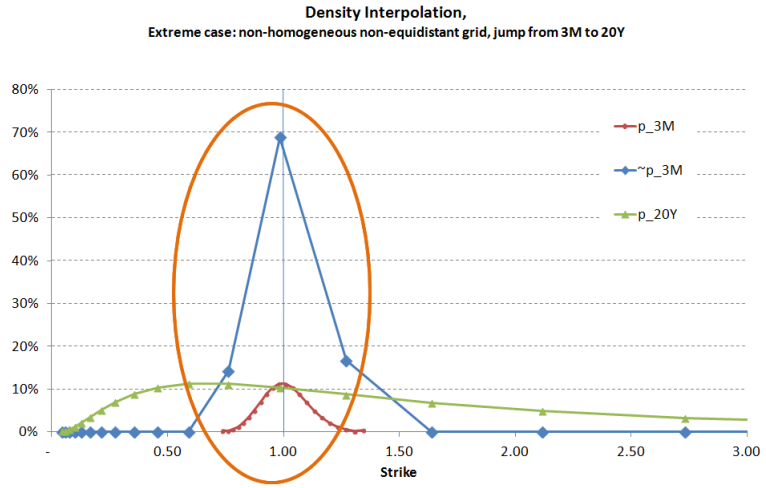

This is simply the result of linear interpolation in call prices when going from p_{3M} to $\tilde{p}_{3M}$, as can be seen from the call prices:

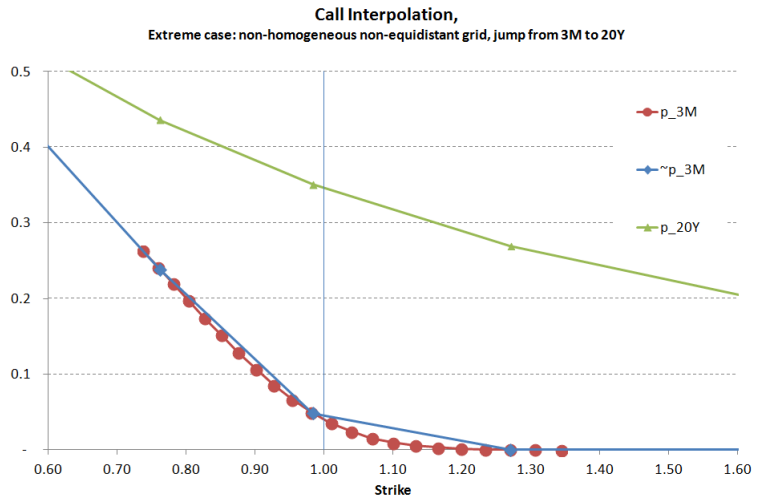

Accordingly, the matrix Ξ which maps p_{3M} onto the much wider strike grid k_{20Y} has the degenerated form:

	0.74	0.76	0.78	0.80	0.83	0.85	0.87	0.90	0.93	0.95	0.98	1.01	1.04	1.07	1.10	1.13	1.16	1.20	1.23	1.27	1.31	1.34
0.05	0%	0%	0%	0%	0%	0%	0%	0%	0%	0%	0%	0%	0%	0%	0%	0%	0%	0%	0%	0%	0%	0%
0.06	0%	0%	0%	0%	0%	0%	0%	0%	0%	0%	0%	0%	0%	0%	0%	0%	0%	0%	0%	0%	0%	0%
0.08	0%	0%	0%	0%	0%	0%	0%	0%	0%	0%	0%	0%	0%	0%	0%	0%	0%	0%	0%	0%	0%	0%
0.10	0%	0%	0%	0%	0%	0%	0%	0%	0%	0%	0%	0%	0%	0%	0%	0%	0%	0%	0%	0%	0%	0%
0.13	0%	0%	0%	0%	0%	0%	0%	0%	0%	0%	0%	0%	0%	0%	0%	0%	0%	0%	0%	0%	0%	0%
0.16	0%	0%	0%	0%	0%	0%	0%	0%	0%	0%	0%	0%	0%	0%	0%	0%	0%	0%	0%	0%	0%	0%
0.21	0%	0%	0%	0%	0%	0%	0%	0%	0%	0%	0%	0%	0%	0%	0%	0%	0%	0%	0%	0%	0%	0%
0.27	0%	0%	0%	0%	0%	0%	0%	0%	0%	0%	0%	0%	0%	0%	0%	0%	0%	0%	0%	0%	0%	0%
0.35	0%	0%	0%	0%	0%	0%	0%	0%	0%	0%	0%	0%	0%	0%	0%	0%	0%	0%	0%	0%	0%	0%
0.46	0%	0%	0%	0%	0%	0%	0%	0%	0%	0%	0%	0%	0%	0%	0%	0%	0%	0%	0%	0%	0%	0%
0.59	14%	2%	0%	0%	0%	0%	0%	0%	0%	0%	0%	0%	0%	0%	0%	0%	0%	0%	0%	0%	0%	0%
0.76	86%	98%	92%	81%	71%	60%	49%	37%	26%	14%	1%	0%	0%	0%	0%	0%	0%	0%	0%	0%	0%	0%
0.98	0%	0%	8%	19%	29%	40%	51%	63%	74%	86%	99%	91%	81%	70%	59%	48%	37%	25%	13%	0%	0%	0%
1.27	0%	0%	0%	0%	0%	0%	0%	0%	0%	0%	0%	9%	19%	30%	41%	52%	63%	75%	87%	100%	90%	80%
1.64	0%	0%	0%	0%	0%	0%	0%	0%	0%	0%	0%	0%	0%	0%	0%	0%	0%	0%	0%	0%	10%	20%
2.12	0%	0%	0%	0%	0%	0%	0%	0%	0%	0%	0%	0%	0%	0%	0%	0%	0%	0%	0%	0%	0%	0%
2.73	0%	0%	0%	0%	0%	0%	0%	0%	0%	0%	0%	0%	0%	0%	0%	0%	0%	0%	0%	0%	0%	0%
3.53	0%	0%	0%	0%	0%	0%	0%	0%	0%	0%	0%	0%	0%	0%	0%	0%	0%	0%	0%	0%	0%	0%
4.56	0%	0%	0%	0%	0%	0%	0%	0%	0%	0%	0%	0%	0%	0%	0%	0%	0%	0%	0%	0%	0%	0%
5.88	0%	0%	0%	0%	0%	0%	0%	0%	0%	0%	0%	0%	0%	0%	0%	0%	0%	0%	0%	0%	0%	0%
7.60	0%	0%	0%	0%	0%	0%	0%	0%	0%	0%	0%	0%	0%	0%	0%	0%	0%	0%	0%	0%	0%	0%
9.81	0%	0%	0%	0%	0%	0%	0%	0%	0%	0%	0%	0%	0%	0%	0%	0%	0%	0%	0%	0%	0%	0%

(note the difference in strike range).

The raw transition matrix I_{20Y} is given as

	0.05	0.06	0.08	0.10	0.13	0.16	0.21	0.27	0.35	0.46	0.59	0.76	0.98	1.27	1.64	2.12	2.73	3.53	4.56	5.88	7.60	9.81
0.05	100%	48%	22%	11%	6%	3%	2%	1%	1%	1%	1%	0%	0%	0%	0%	0%	0%	0%	0%	0%	0%	0%
0.06	0%	32%	14%	7%	4%	2%	1%	1%	1%	0%	0%	0%	0%	0%	0%	0%	0%	0%	0%	0%	0%	0%
0.08	0%	14%	43%	21%	11%	6%	4%	2%	2%	1%	1%	1%	1%	0%	0%	0%	0%	0%	0%	0%	0%	0%
0.10	0%	4%	14%	40%	21%	12%	7%	5%	3%	2%	2%	1%	1%	1%	1%	0%	0%	0%	0%	0%	0%	0%
0.13	0%	1%	5%	13%	37%	21%	13%	8%	6%	4%	3%	3%	2%	2%	1%	1%	1%	0%	0%	0%	0%	0%
0.16	0%	1%	2%	5%	13%	34%	20%	13%	9%	7%	5%	4%	3%	3%	2%	1%	1%	1%	0%	0%	0%	0%
0.21	0%	0%	1%	2%	5%	13%	31%	20%	14%	10%	8%	6%	5%	4%	3%	2%	1%	1%	0%	0%	0%	0%
0.27	0%	0%	0%	1%	2%	5%	12%	27%	19%	14%	11%	9%	7%	5%	4%	3%	2%	1%	1%	0%	0%	0%
0.35	0%	0%	0%	0%	1%	2%	5%	12%	24%	18%	14%	11%	9%	7%	5%	3%	2%	1%	1%	0%	0%	0%
0.46	0%	0%	0%	0%	0%	1%	2%	5%	11%	21%	16%	13%	10%	8%	6%	4%	3%	2%	1%	1%	0%	0%
0.59	0%	0%	0%	0%	0%	0%	1%	2%	5%	9%	18%	14%	11%	9%	6%	4%	3%	2%	1%	1%	0%	0%
0.76	0%	0%	0%	0%	0%	0%	0%	1%	2%	4%	8%	14%	11%	9%	6%	4%	3%	2%	1%	1%	0%	0%
0.98	0%	0%	0%	0%	0%	0%	0%	0%	1%	2%	4%	7%	11%	9%	6%	4%	3%	2%	1%	1%	0%	0%
1.27	0%	0%	0%	0%	0%	0%	0%	0%	1%	1%	3%	5%	8%	14%	10%	7%	5%	3%	2%	1%	0%	0%
1.64	0%	0%	0%	0%	0%	0%	0%	0%	1%	1%	2%	4%	7%	11%	17%	12%	8%	5%	3%	2%	1%	0%
2.12	0%	0%	0%	0%	0%	0%	0%	0%	0%	1%	2%	3%	5%	8%	12%	21%	14%	8%	5%	3%	1%	0%
2.73	0%	0%	0%	0%	0%	0%	0%	0%	0%	1%	1%	2%	3%	5%	8%	14%	24%	15%	9%	5%	2%	0%
3.53	0%	0%	0%	0%	0%	0%	0%	0%	0%	0%	1%	1%	2%	3%	5%	8%	15%	27%	16%	9%	4%	0%
4.56	0%	0%	0%	0%	0%	0%	0%	0%	0%	0%	0%	1%	1%	2%	3%	5%	8%	15%	30%	17%	8%	0%
5.88	0%	0%	0%	0%	0%	0%	0%	0%	0%	0%	0%	0%	1%	1%	2%	3%	4%	8%	16%	33%	17%	0%
7.60	0%	0%	0%	0%	0%	0%	0%	0%	0%	0%	0%	0%	0%	0%	0%	0%	1%	1%	3%	5%	12%	0%
9.81	0%	0%	0%	0%	0%	0%	0%	0%	0%	0%	0%	0%	0%	1%	1%	2%	3%	5%	11%	23%	51%	100%

The transition kernel $\Pi_{20Y} = I_{20Y}\Xi_{20Y}$ from $\tilde{p}_{3M}$ to p_{20Y} is therefore given as follows:

	0.74	0.76	0.78	0.80	0.83	0.85	0.87	0.90	0.93	0.95	0.98	1.01	1.04	1.07	1.10	1.13	1.16	1.20	1.23	1.27	1.31	1.34
0.05	0%	0%	0%	0%	0%	0%	0%	0%	0%	0%	0%	0%	0%	0%	0%	0%	0%	0%	0%	0%	0%	0%
0.06	0%	0%	0%	0%	0%	0%	0%	0%	0%	0%	0%	0%	0%	0%	0%	0%	0%	0%	0%	0%	0%	0%
0.08	1%	1%	1%	1%	1%	1%	1%	1%	1%	1%	1%	1%	1%	1%	1%	1%	1%	1%	1%	0%	0%	0%
0.10	2%	2%	1%	1%	1%	1%	1%	1%	1%	1%	1%	1%	1%	1%	1%	1%	1%	1%	1%	1%	1%	1%
0.13	3%	3%	3%	3%	2%	2%	2%	2%	2%	2%	2%	2%	2%	2%	2%	2%	2%	2%	2%	2%	2%	2%
0.16	4%	4%	4%	4%	4%	4%	4%	4%	4%	4%	3%	3%	3%	3%	3%	3%	3%	3%	3%	3%	3%	2%
0.21	7%	6%	6%	6%	6%	6%	6%	6%	5%	5%	5%	5%	5%	5%	5%	4%	4%	4%	4%	4%	4%	4%
0.27	9%	9%	9%	8%	8%	8%	8%	8%	7%	7%	7%	7%	7%	6%	6%	6%	6%	6%	6%	5%	5%	5%
0.35	12%	11%	11%	11%	10%	10%	10%	10%	9%	9%	9%	9%	8%	8%	8%	8%	8%	7%	7%	7%	7%	6%
0.46	14%	13%	13%	13%	12%	12%	12%	11%	11%	11%	10%	10%	10%	10%	9%	9%	9%	9%	8%	8%	8%	8%
0.59	15%	14%	14%	14%	13%	13%	13%	12%	12%	12%	11%	11%	11%	10%	10%	10%	10%	9%	9%	9%	8%	8%
0.76	13%	14%	14%	14%	13%	13%	13%	12%	12%	12%	11%	11%	11%	10%	10%	10%	10%	9%	9%	9%	8%	8%
0.98	6%	7%	7%	8%	8%	9%	9%	10%	10%	11%	11%	11%	11%	11%	10%	10%	10%	9%	9%	9%	9%	8%
1.27	5%	5%	5%	6%	6%	6%	7%	7%	8%	8%	8%	9%	9%	10%	11%	11%	12%	12%	13%	14%	13%	13%
1.64	4%	4%	4%	4%	5%	5%	5%	6%	6%	6%	7%	7%	7%	8%	8%	9%	9%	10%	10%	11%	11%	12%
2.12	3%	3%	3%	3%	3%	4%	4%	4%	4%	4%	5%	5%	5%	6%	6%	6%	7%	7%	7%	8%	8%	9%
2.73	2%	2%	2%	2%	2%	2%	3%	3%	3%	3%	3%	3%	4%	4%	4%	4%	4%	5%	5%	5%	5%	6%
3.53	1%	1%	1%	1%	1%	1%	2%	2%	2%	2%	2%	2%	2%	2%	2%	3%	3%	3%	3%	3%	3%	4%
4.56	1%	1%	1%	1%	1%	1%	1%	1%	1%	1%	1%	1%	1%	1%	1%	1%	2%	2%	2%	2%	2%	2%
5.88	0%	0%	0%	0%	0%	0%	0%	0%	1%	1%	1%	1%	1%	1%	1%	1%	1%	1%	1%	1%	1%	1%
7.60	0%	0%	0%	0%	0%	0%	0%	0%	0%	0%	0%	0%	0%	0%	0%	0%	0%	0%	0%	0%	0%	0%
9.81	0%	0%	0%	0%	0%	0%	0%	0%	0%	0%	0%	0%	0%	0%	0%	1%	1%	1%	1%	1%	1%	1%

4.6 Worked Example: Pricing Bermudan Digitals

In this section we present some results on using the model to price exotic options, and its dependence on its key parameters. To this end, we calibrate the model to SPX on October 2nd, 2015 to a strike grid given by formula (8) on page 11, with the additional ability to separate between downside and upside "standard deviation" δ.

We then use the backward induction scheme presented in section 4 pg. 22ff. to price three product types, each with a two year maturity: plain vanilla calls, Bermudan KO digitals whose barrier is observed every 3M, and American KO digitals.

The model parameters we are interested in are: changes to the number of strikes, changes to the standard deviations in (8), and finally changes to the number of intermediate calibration times – i.e., what is the impact of calibrating the model to time steps $(t_j)_j$ every day, every second day, every week, every month or every three months.

Vanilla Calls

The following graphs show the impact of change the pricing parameters on pricing 2Y vanilla calls. Predictably, the impact is tiny as it only affects the interpolation of the call between the closest strikes used at the 2Y maturity point. This example has been included as sanity check.

The first graph shows the effect of decreasing time steps from three months down to one day:

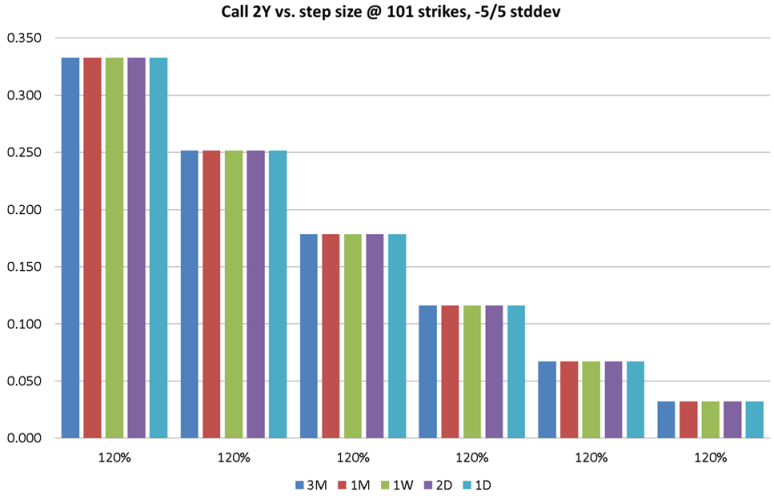

The second graph shows the effect of changing the number of strikes used to interpolate call prices:

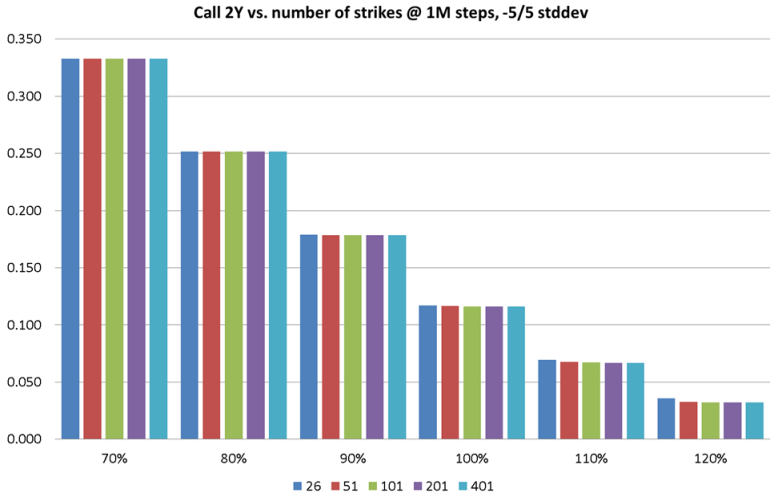

The final graph shows the effect of changing downside ("-") and upside ("+") standard deviations:

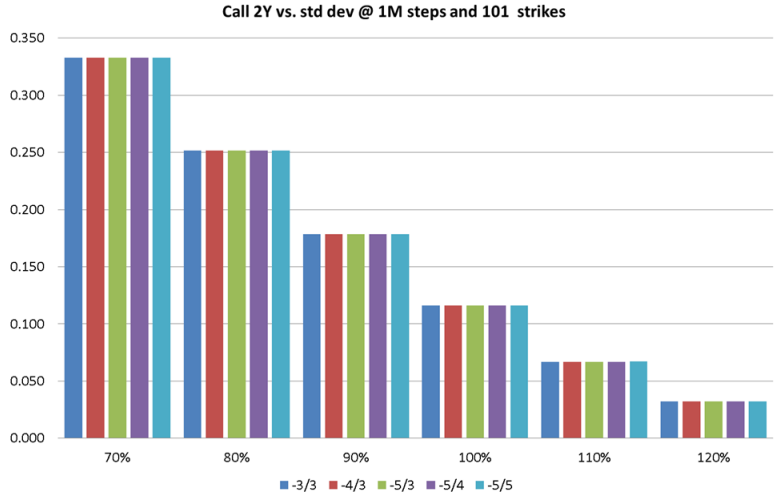

3M Bermudan Digitals

We now consider 3M Bermudan KO digitals, i.e. a product which pays 1 in two years if the barrier has not been reached between now and maturity at any one of the quarterly observations. A barrier above 100% is considered an up-and-out barrier, while a barrier below 100% is considered a down-and-out barrier.

The first observation is that increasing the frequency of the calibration *does* affect the price of the Bermudan. That is expected, since our model is not-self similar in the sense that if we calibrate it to t_1, t_3 only, and then to t_1, t_1, t_3, then the conditional distributions between t_1 and t_3 are not the same.

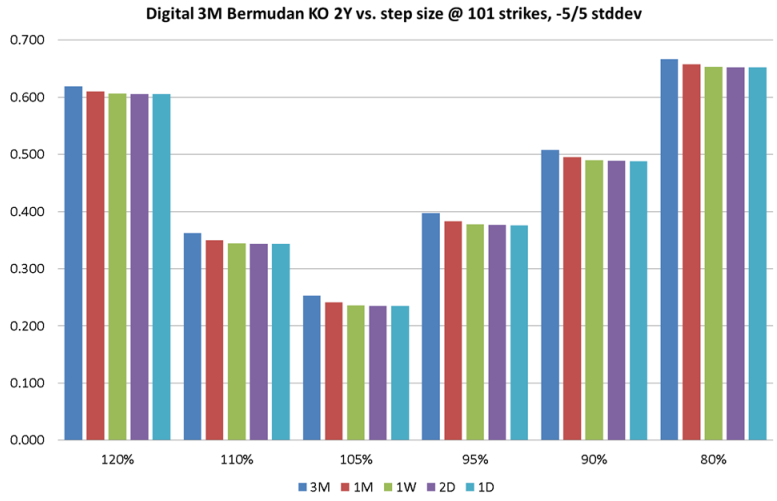

However, the impact remains within typical noise levels for this kind of pricing schemes. The result suggests as a generic calibration scheme to first always

calibrate to all maturities with quoted option prices, and then to insert regular one-month steps to improve robustness.

To confirm this approach, we have also priced a 5Y Bermudan Digital with a 6M observation frequency. The model converged again well with monthly steps.

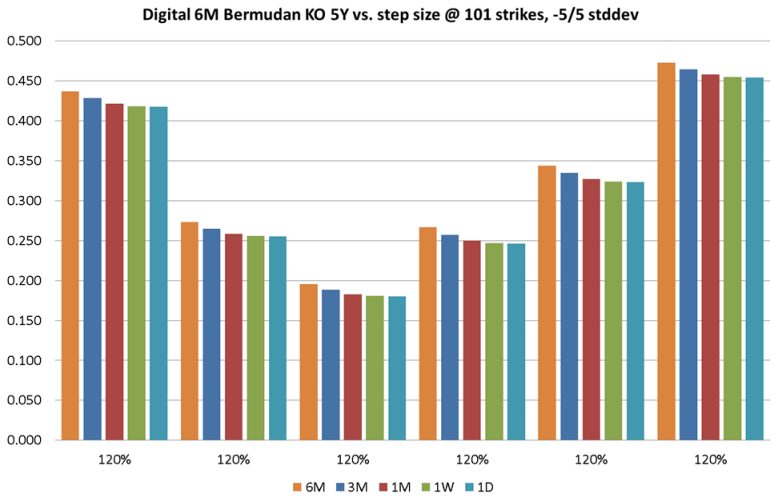

The next graph shows the effect of changes to the number of strikes used. There has been no attempt to optimize the strikes as it is common for Finite Difference schemes (i.e., placing fixed node points right around the barrier). The result is again satisfactory and shows that even with very a modest 51 strikes per maturity the model converges well:

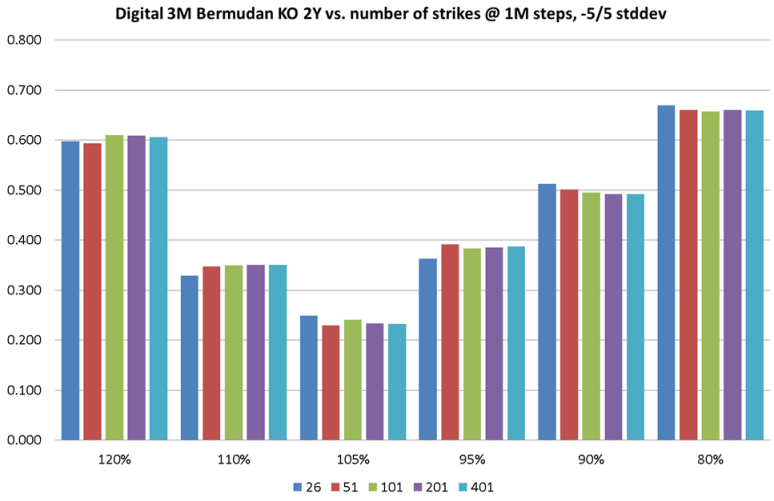

Finally, we observe a similar level of noise by changing the width of the strike range. The graph shows changing downside ("-") and upside ("+") standard

deviations. The presence of a high skew in the SPX on October 2nd, 2015 means that we have to use quite a wide strike range to capture the distribution well — downside Bermudans are more affected by changing the interpolation width than upside barriers.

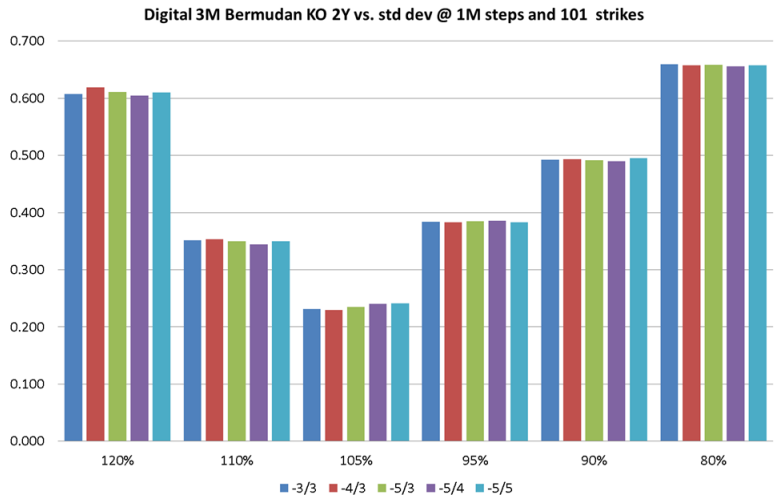

American Digitals

We now repeat our experiment with an American Digital where the barrier is tested at every observation point. The big difference to our previous examples is that increasing the step size for the model now also increases the observation frequency for the American barrier: if the model is calibrated to 3M, then it would only test the American barrier at those maturities. In other words, the graph really shows the convergence of pricing an American barrier with brute force approximation of the Bermudan barriers. Accordingly, convergence is slow as expected.

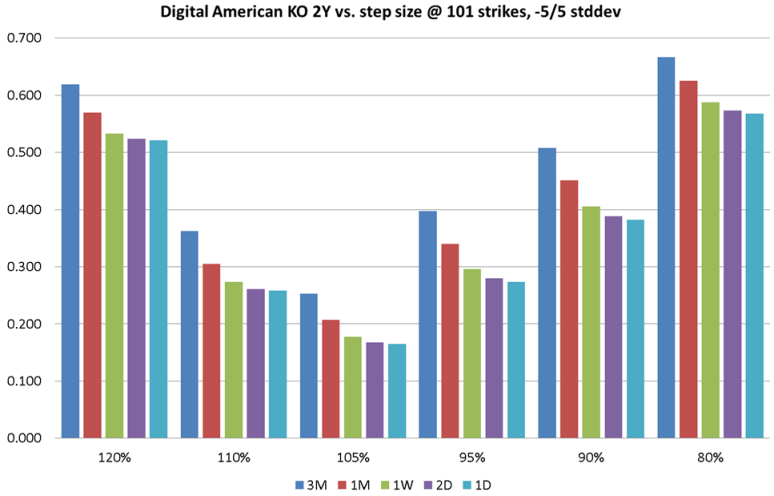

Predictably, that means that if the model is used to price continuous or daily barriers, then it practically becomes a local volatility model – there is no advantage of taking large steps. While the model can still be calibrated efficiently, it will be slower to compute than local volatility if the market itself is already arbitrage-free. This can be avoided by calibrating the model to a lower frequency such as one month steps, and to then employ an ad-hoc interpolation scheme between maturities which again allows efficient pricing even with daily observations.

5 Summary

We have shown how to use linear programs to find option surface which are *globally* L^1-closest to a given input option surface, which admit a bounded discrete "Backward Local Volatility", and for which we can construct unconditionally consistent transition probability kernels using, effectively, implicit FD operator matrices.

These can then be used to drive forward and backward induction schemes or Monte-Carlo simulations, all of which are fully consistent with the calibration option price surface. We have presented a few examples of using backward induction schemes.

A Appendix

A.1 Approximation of Derivatives on Non-Equidistant Grids

Assume that we are given strike $k_- < k_0 < k_+$. We wish to define a second order approximation of the first and second order derivatives of a function f, $f' \equiv f'(k_0)$ and $f'' \equiv f''(k_0)$ over these strikes. Let f_+, f_0, f_- be the respective

function values on the strikes. Also define $dk_\pm := \pm(k_\pm - k_0)$ and $df_\pm := \pm(f_\pm - f_0)$. Second order Taylor gives the two equations

$$\begin{aligned}
&\begin{cases} f_+ &\approx f_0 + f'dk_+ + \frac{1}{2}f''dk_+^2 \\ f_- &\approx f_0 - f'dk_- + \frac{1}{2}f''dk_-^2 \end{cases} \\
\Leftrightarrow\quad &\begin{cases} f_+ - f_0 &\approx f'dk_+ + \frac{1}{2}f''dk_+^2 \\ f_0 - f_- &\approx f'dk_- - \frac{1}{2}f''dk_-^2 \end{cases} \\
\Leftrightarrow\quad &\begin{cases} \frac{df_+}{dk_+} - f' &\approx +\frac{1}{2}f''dk_+ \\ \frac{df_-}{dk_-} - f' &\approx -\frac{1}{2}f''dk_- \end{cases}
\end{aligned}$$

From this, we obtain first

$$\frac{df_+}{dk_+} - \frac{df_-}{dk_-} \approx \frac{1}{2}(dk_+ + dk_-)f''$$

i.e. the second order approximation for the second derivative is

$$f'' \approx \frac{dk_- f_+ - (dk_+ + dk_-)f_0 + dk_+ f_-}{\frac{1}{2}(dk_+ + dk_-)dk_+dk_-} \ .$$

For the first order, let

$$\begin{cases} \frac{df_+}{dk_+^2} - \frac{f'}{dk_+} &\approx +\frac{1}{2}f'' \\ \frac{df_-}{dk_-^2} - \frac{f'}{dk_-} &\approx -\frac{1}{2}f'' \ , \end{cases}$$

such that

$$df_+ \frac{dk_-^2}{dk_+^2 dk_-^2} + df_- \frac{dk_+^2}{dk_+^2 dk_-^2} \approx f' \frac{dk_+ + dk_-}{dk_+ dk_-} \ .$$

This yields the second order approximation for the first derivative as

$$f' \approx \frac{dk_-^2 f_+ + (dk_+^2 - dk_-^2)f_0 - dk_+^2 f_-}{(dk_+ + dk_-)dk_+dk_-} \ .$$

A.2 Proofs

Proof of theorem 3.1 and corollary 3.1– we reiterate the proof in [Bu06]: we first show that p_j is a probability density. We drop the index j for the proof.

For $i = 0, \ldots, n-1$, corollary 3.1 shows that $p^i = \frac{1}{2}(dk_+^i + dk_-^i)\Gamma^i$, hence *3.* implies that those p^i are positive. Since $\Delta^{n-1} \leq 0$, $p^n = -\Delta^{n-1}$ is positive, too, while $\Delta_j^{-1} \geq -1$ implies $p^{-1} = \Delta^{-1} + 1 \geq 0$.

To show that the probabilities all add up to 1, note

$$\sum_{i=-1}^{n} p^i = \left(\Delta^n - \Delta^{-1}\right) + \left(\Delta^{-1} + 1\right) = 1 \ .$$

We now show that the expected value of the random variable is 1, as claimed. To this end

$$\begin{aligned}
\sum_{i=-1}^{n} k^i p^i &= \sum_{i=0}^{n} k^i(\Delta^i - \Delta^{i-1}) + k^{-1}(1+\Delta^{-1}) \\
&= \sum_{\ell=0}^{n-1}(k^\ell - k^{\ell+1})\Delta^\ell + k^n\Delta^n - k^0\Delta^{-1} + k^{-1}(1+\Delta^{-1}) \\
&= \sum_{\ell=-1}^{n-1}(k^\ell - k^{\ell+1})\Delta^\ell + k^{-1} \\
&= \sum_{\ell=-1}^{n-1}(C^\ell - C^{\ell+1}) + k^{-1} \\
&= C^{-1} - C^n + k^{-1} \\
&= 1
\end{aligned}$$

Next, we will show representation (6). To this end, chose an arbitrary strike k^r. For $r = n$ our equation obviously holds. Assume therefore $-1 \leq r < n$.

$$\begin{aligned}
\sum_{i=0}^{n}(k^i - k^r)^+ p^i &= \left(\sum_{i=r+1}^{n} k^i p^i\right) - k^r\left(\sum_{i=r+1}^{n} p^i\right) \\
&= \sum_{i=r+1}^{n} k^i(\Delta^i - \Delta^{i-1}) - k^r\left(\Delta^n - \Delta^r\right) \\
&= \sum_{\ell=r+1}^{n-1}(k^\ell - k^{\ell+1})\Delta^\ell + k^n\Delta^n - k^{r+1}\Delta^r - k^r\left(\Delta^n - \Delta^r\right) \\
&= \sum_{\ell=r}^{n-1}(C^\ell - C^{\ell+1}) \\
&= C^r \ ,
\end{aligned}$$

as claimed. □

Proof of theorem 4.1– Let X be a diffusion satisfying

$$dX_t = \mu_t(X_t)\,dt + \sigma_t^2(X_t)\,dW_t$$

and which has unattainable boundaries $\ell \in [-\infty, \infty)$ and $u \in (\ell, \infty]$. The means that for any sufficiently smooth and bounded function f,

$$\int_\ell^u \partial_x f(x) p_t(x)\,dx = -\int_\ell^u f(x)\partial_x p_t(x)\,dx + \underbrace{|f(x)p_t(x)|_\ell^u}_{=0} \ . \tag{43}$$

Let $f_t(x) := \mathbb{E}[f(X_T)|X_t = x]$ for a smooth "test function" f with compact support (hence bounded), and assume that μ and σ are sufficiently regular such that

$$0 = \partial_t f_t(x) + \mathcal{L}_t(x) f_t(x) \ , \quad \mathcal{L}_t(x) := \mu_t(x)\,\partial_x + \frac{1}{2}\sigma_t^2(x)\,\partial_{xx}^2 \ .$$

We also have the expectation operator $f' p_t := \mathbb{E}\,[\,f(X_t)\,]$. Applying it to our PDE gives

$$\begin{aligned} 0 &= \mathbb{E}\,[\,\partial_t f_t(X_t) + \mathcal{L}_t(X_t) f_t(X_t)\,] \\ &= (\partial_t f_t)'\, p_t + \left(\mathcal{L}_t f_t\right)' p_t \\ &\overset{(43)}{=} f_t'\,(\partial_t' p_t) + f_t'\left(\mathcal{L}_t' p_t\right) \ . \end{aligned}$$

Since f and T were arbitrary, this implies Lebesgue-almost surely that

$$0 = -\partial_t p_t + \mathcal{L}_t' p_t \ ,$$

Lebesgue-almost surely, as claimed. □

Example 1 *Let*

$$dX_t = \kappa(\Xi - X_t)\,dt + \sigma\sqrt{X_t}\,dW_t$$

and assume that zero is attainable, i.e. the "Feller condition" is violated.

Then, X does not have compact support and backward and forward operators are not the adjoint of each other.

References

[AH10] *J.Andreasen, B.Huge:*
"Volatility Interpolation", Risk March 2011
`http://ssrn.com/abstract=1694972`

[AH11] *J.Andreasen, B.Huge:*
"Random Grids", Risk 24.7 (Jul 2011): 62-67.

[BR94] *A.Berman, R.Plemmons:*
Nonnegative Matrices in the Mathematical Sciences, Society for Industrial and Applied Mathematics; Rev Ed edition, 1994

[Ba96] *D.Bates:*
"Jumps and stochastic volatility: exchange rate process implicit in DM options", Rev. Fin. Studies 9-1, 1996

[Bu06] *H.Buehler*:
"Expensive Martingales", Quantitative Finance, Vol. 6, No. 3, June 2006,
`http://ssrn.com/abstract=1118246`

[Bu10] *H.Buehler*:
"Volatility and Dividends - Volatility Modelling with Cash Dividends and Simple Credit Risk", WP February 2, 2010
`http://ssrn.com/abstract=114187`

[Bu11] *H.Buehler*:
"Stochastic Dividend Modeling", presentation, Global Derivatives Trading & Risk Management Conference Paris, Thursday April 14th, 2011
`http://quantitative-research.de/dl/ModellingDividends.pdf`

[BG16] *H.Buehler, E.Ryskin*:
"Discrete Local Volatility", presentation, Global Derivatives Trading & Risk Management Conference Paris, Wednesday May 11th, 2016
`http://quantitative-research.de/dl/DiscreteLocalVol.pdf`

[DK94] *E.Derman, I.Kani:*
"The Volatility Smile and Its Implied Tree", Goldman Sachs Quantitative Strategies Research Notes, 1994

[Du96] *B.Dupire:*
"Pricing with a Smile", Risk, 7 (1), pp. 18-20, 1996

[Ga06] *J.Gatheral:*
"The Volatility Surface: A Practitioner's Guide", Wiley 2006

[Gl04] *P.Glasserman:*
Monte carlo methods in financial engineering, Springer, 2004

[He93] *S.Heston:*
"A closed-form solution for options with stochastic volatility with applications to bond and currency options", Review of Financial Studies, 1993.

[KP11] *P.Kloeden, E.Platen:*
Numerical Solution of Stochastic Differential Equations (Stochastic Modelling and Applied Probability), Springer; 1992. Corr. 4th edition (15 Jun. 2011)